$NNLO_{sat}$ and predictions for light- and medium-mass nuclei

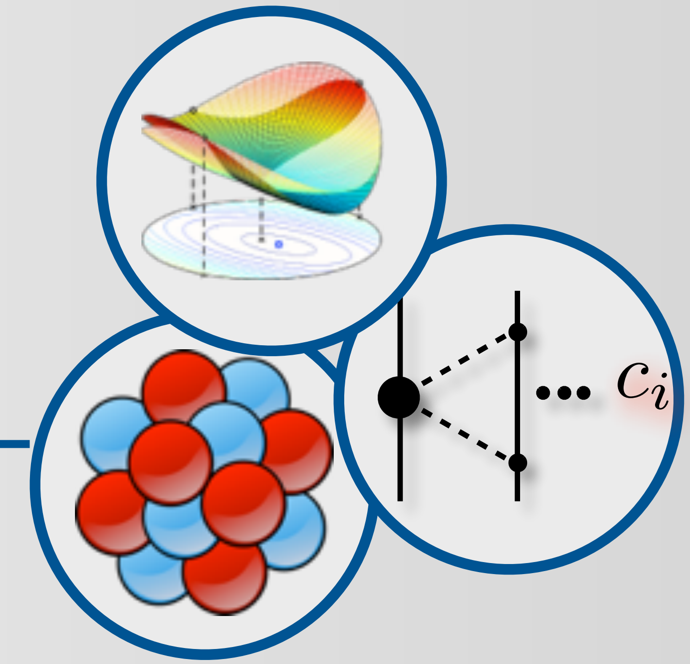

Andreas Ekström (UT/ORNL)

Collaborators:
Boris Carlsson (UiO/Chalmers)
Christian Forssén(Chalmers)
Gaute Hagen(UT/ORNL)
Morten Hjorth-Jensen(UiO/MSU)
Gustav Jansen(UT/ORNL)
Petr Navrátil (TRIUMF)
Witold Nazarewicz(MSU/UT/ORNL)
Thomas Papenbrock(UT/ORNL)
Kyle Wendt(UT/ORNL)

Progress in Ab Initio Techniques in Nuclear Physics, February 17-20, 2015, TRIUMF, Vancouver, BC, Canada

- *Motivation and introduction*
- *The $NNLO_{sat}$ optimization*
- *Light- and medium-mass nuclei*
- *Symmetric nuclear matter*
- *Summary and conclusions*

Motivation and Introduction

- In several cases the numerical solution of the many-body Schrödinger equation is no longer the bottleneck for accurate results/predictions in nuclear modeling, instead it is the input nuclear interaction.

- Currently, chiral nuclear interactions systematically overbind atomic nuclei and predict too small charge radii. These discrepancies increase with mass number.

- This is a serious shortcoming. There are no accurate ab initio calculations of the proton/neutron distributions in atomic nuclei.

- Therefore we have optimized the LECs of the NN+3NF interaction at next-to-next-to leading-order (NNLO) to low-energy *scattering data as well as binding energies and radii in selected psd-shell nuclei:*

  arXiv: 1502.04682 [nucl-th]

- There are many exciting experimental efforts that are directly linked to the neutron physics in medium- and heavy-mass isotopes, e.g. CREX and PREX at Jefferson Lab.

NNLO$_{sat}$: a quantitative NNLO interaction

LO

NLO

NNLO

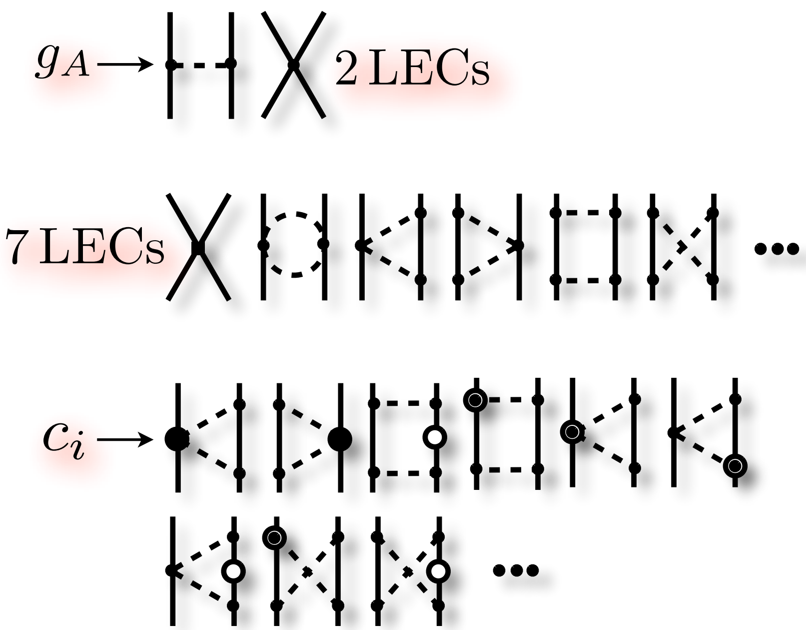

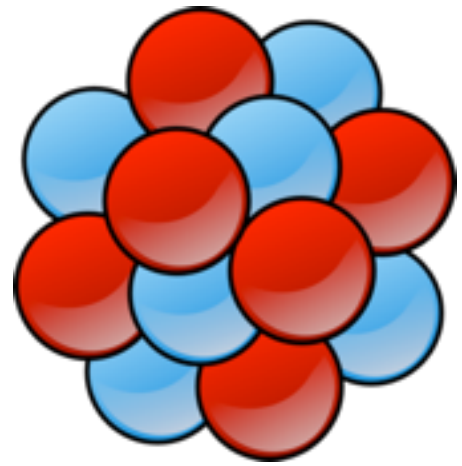

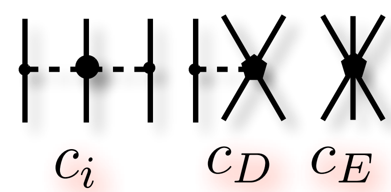

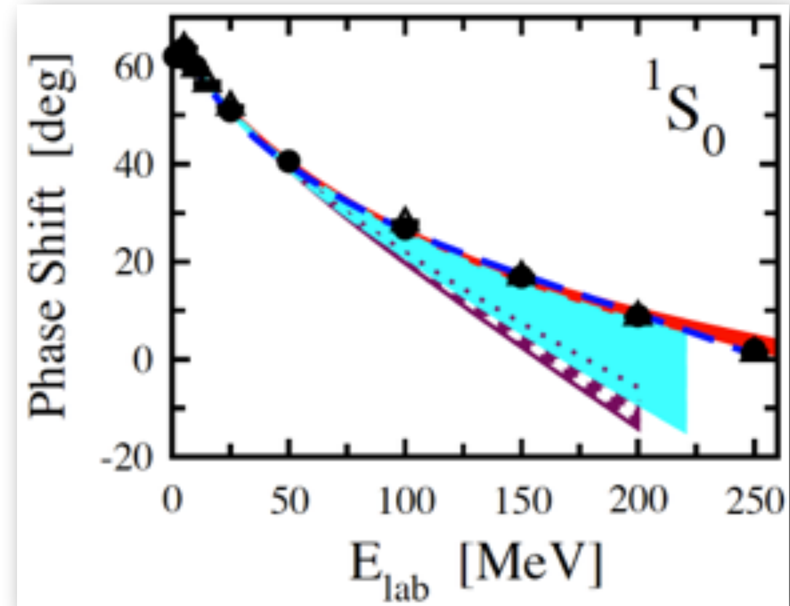

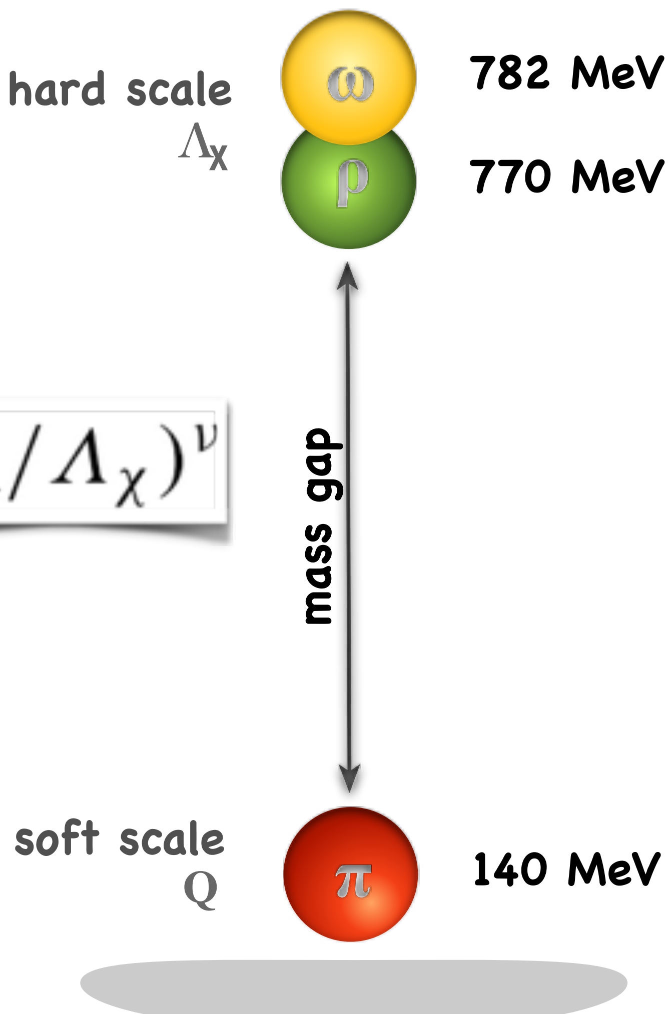

$$(Q/\Lambda_\chi)^\nu$$

Chiral EFT

QCD-symmetries, scale separation, expansion in soft-scale/hard-scale

Modern nuclear forces are based on chiral EFT: e.g. idaho-N3LO (500).
quantitative studies feasible at NNLO (~twice as many LECs at N3LO)

Still many unresolved issues:
- order-by-order convergence
- uncertainties
- cutoff dependence
- power counting

Christian Forssen

+ many other contributions on chiral EFT at this workshop

E. Epelbaum et al. Rev. Mod. Phys. 81, 1773 (2009)
R. Machleidt et al. Phys. Rep. 503, 1 (2011)

Current situation

- We have N2LO and N3LO high-precision NN potentials. (χ^2/datum=1)
- Accompanying 3NF interactions have been tuned separately.
- Non-local 3NFs have so far provided better results than local ones.

Current situation

- We have N2LO and N3LO high-precision NN potentials. (χ^2/datum=1)
- Accompanying 3NF interactions have been tuned separately.
- Non-local 3NFs have so far provided better results than local ones.

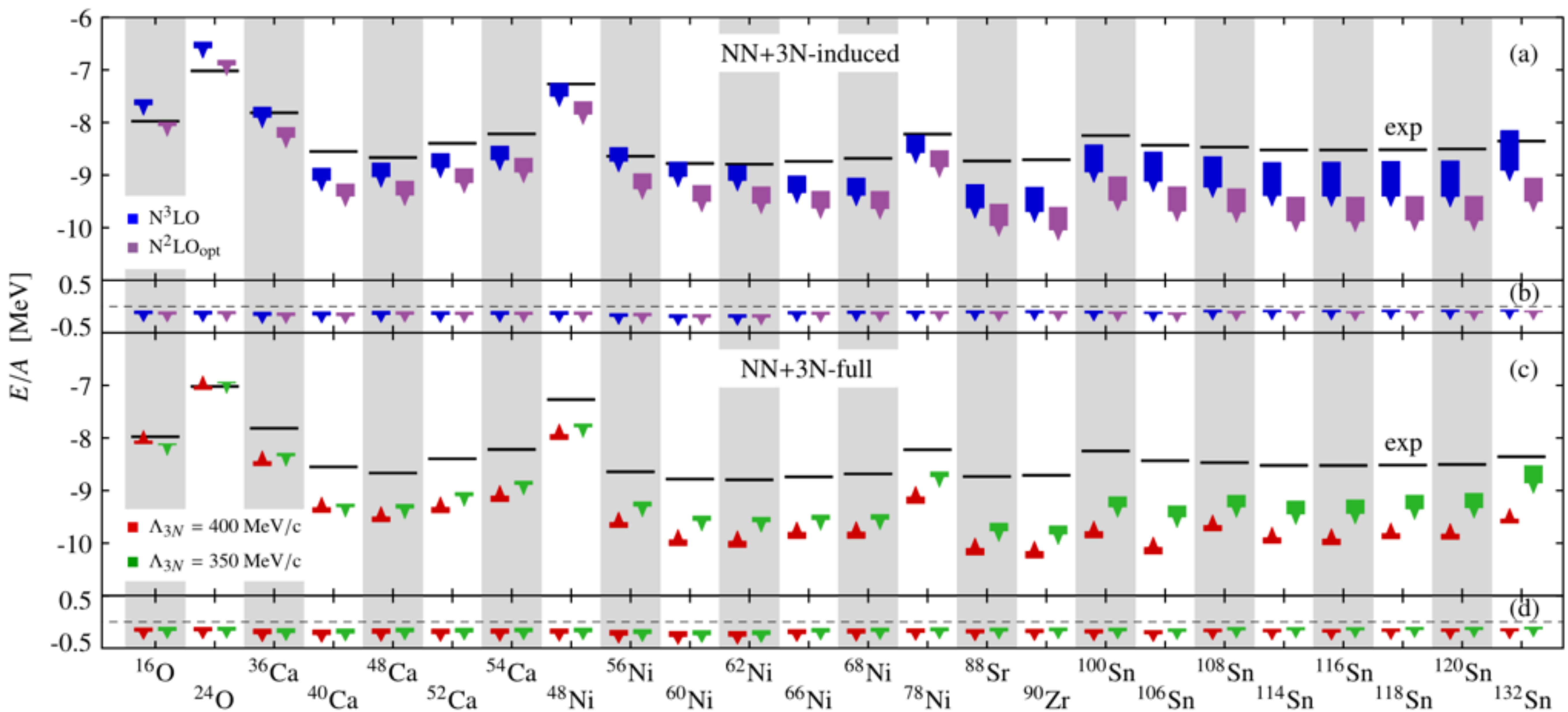

S. Binder et al. Phys. Lett. B 736, 119 (2014)

Current situation

- We have N2LO and N3LO high-precision NN potentials. (χ^2/datum=1)
- Accompanying 3NF interactions have been tuned separately.
- Non-local 3NFs have so far provided better results than local ones.

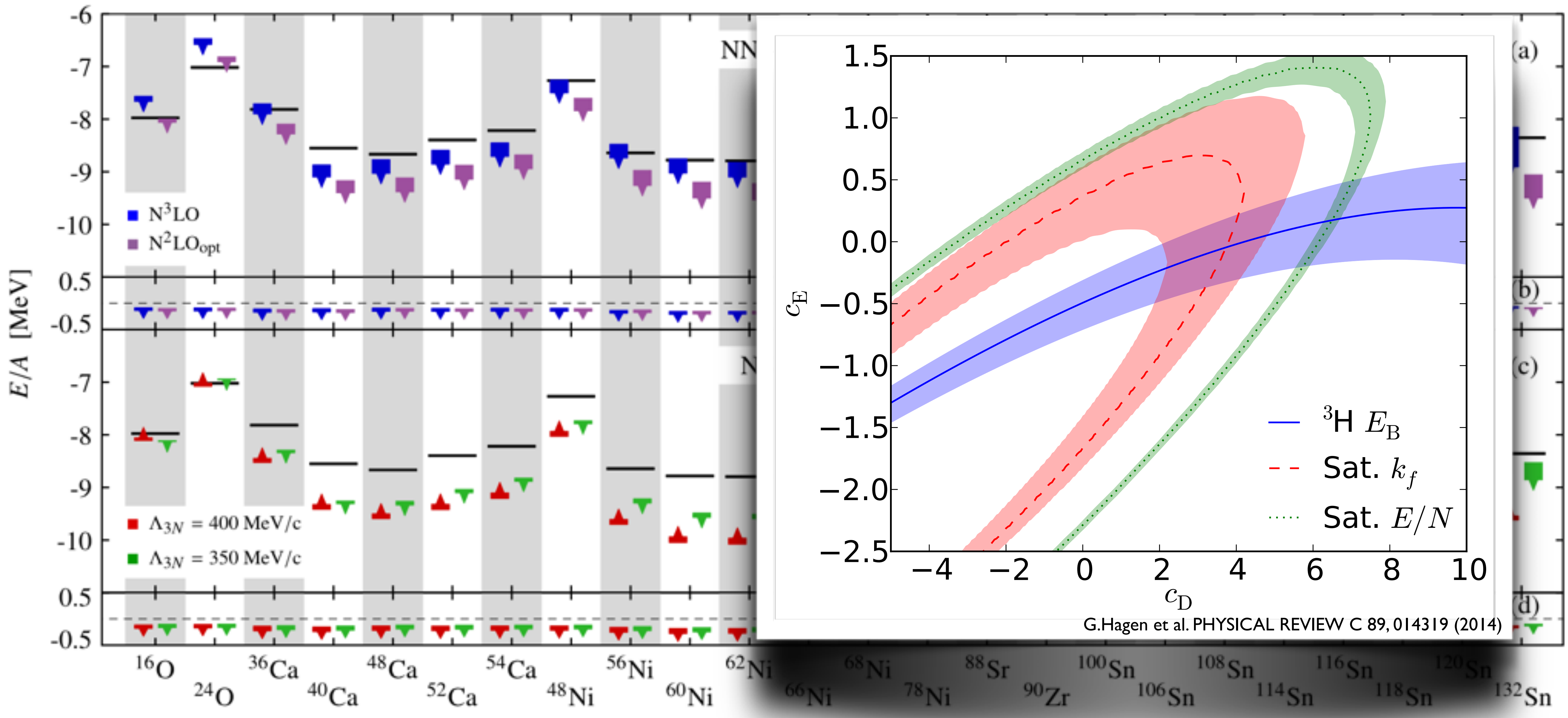

S. Binder et al. Phys. Lett. B 736, 119 (2014)

NNLO$_{\text{sat(uration)}}$ and *"in-medium optimization"*: design

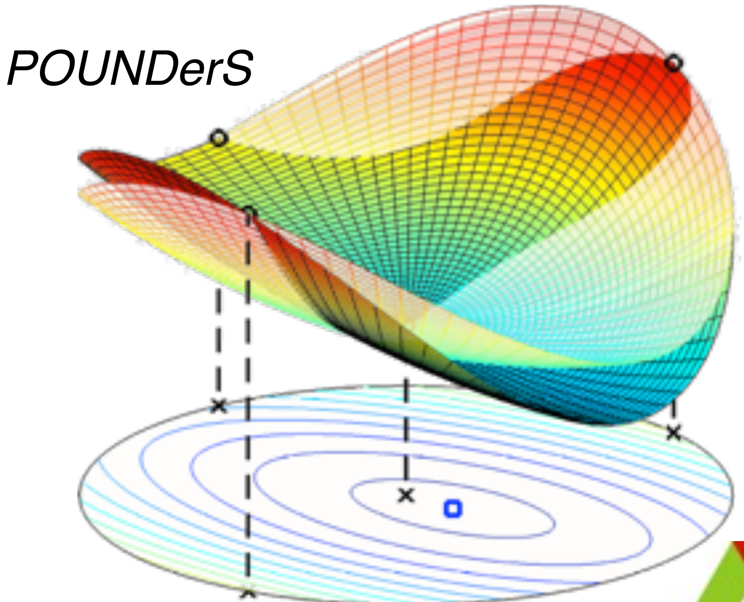

Argonne NATIONAL LABORATORY

Interaction: NN+3NF(non-local) NNLO cutoff=450 MeV

Optimization: vary all LECs in NN+3NF simultaneously

Design goal: describe binding energies and radii for A=2, 3, 4, p-shell, and sd-shell

$$\min_{\vec{x}} \left[f(\vec{x}) = \sum_{q=1}^{N} \left(\frac{O(\vec{x})_q - O_q^{\exp}}{w_q} \right)^2 \right]$$

NNLO$_{\mathrm{sat(uration)}}$ and *"in-medium optimization"*: *design*

POUNDerS

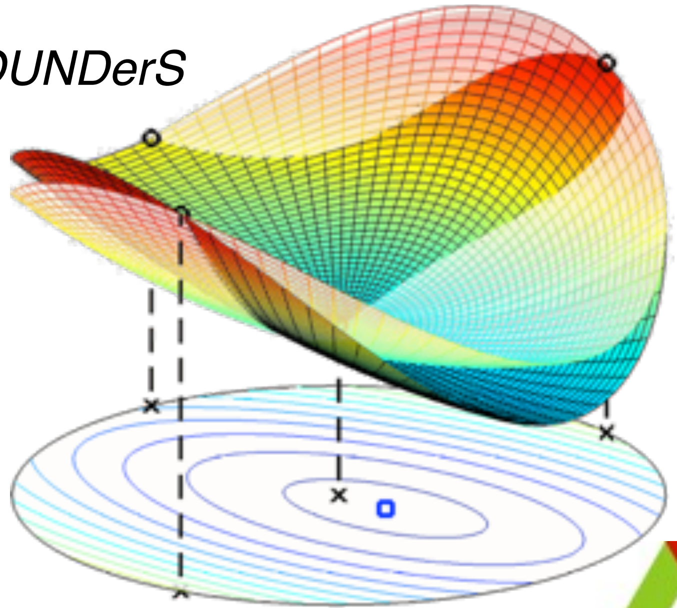

Argonne NATIONAL LABORATORY

Interaction: NN+3NF(non-local) NNLO cutoff=450 MeV

Optimization: vary all LECs in NN+3NF simultaneously

Design goal: describe binding energies and radii for A=2, 3, 4, p-shell, and sd-shell

$$\min_{\vec{x}} \left[f(\vec{x}) = \sum_{q=1}^{N} \left(\frac{O(\vec{x})_q - O_q^{\mathrm{exp}}}{w_q} \right)^2 \right]$$

Nucleon-nucleon scattering data up to Tlab=35 MeV

Scattering lengths and effective ranges in the $^1S_0$ channels

NCSM and CCSD(Nmax=8) solutions of binding energies and charge radii for a selected set of light nuclei

$\text{NNLO}_{\text{sat(uration)}}$ and *“in-medium optimization”: design*

POUNDerS

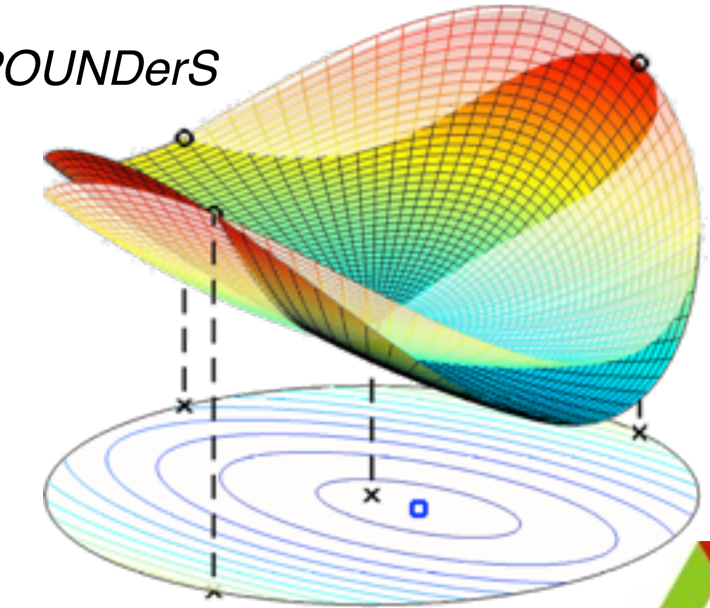

Argonne NATIONAL LABORATORY

Interaction: NN+3NF(non-local) NNLO cutoff=450 MeV

Optimization: vary all LECs in NN+3NF simultaneously

Design goal: describe binding energies and radii for A=2, 3, 4, p-shell, and sd-shell

$$\min_{\vec{x}} \left[f(\vec{x}) = \sum_{q=1}^{N} \left(\frac{O(\vec{x})_q - O_q^{\exp}}{w_q} \right)^2 \right]$$

Nucleon-nucleon scattering data up to Tlab=35 MeV

Scattering lengths and effective ranges in the $^1S_0$ channels

NCSM and CCSD(Nmax=8) solutions of binding energies and charge radii for a selected set of light nuclei

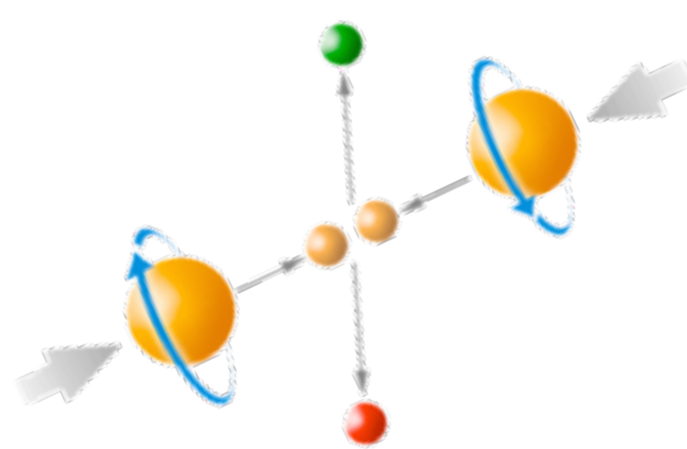

NNLO$_{sat(uration)}$ and *"in-medium optimization"*: design

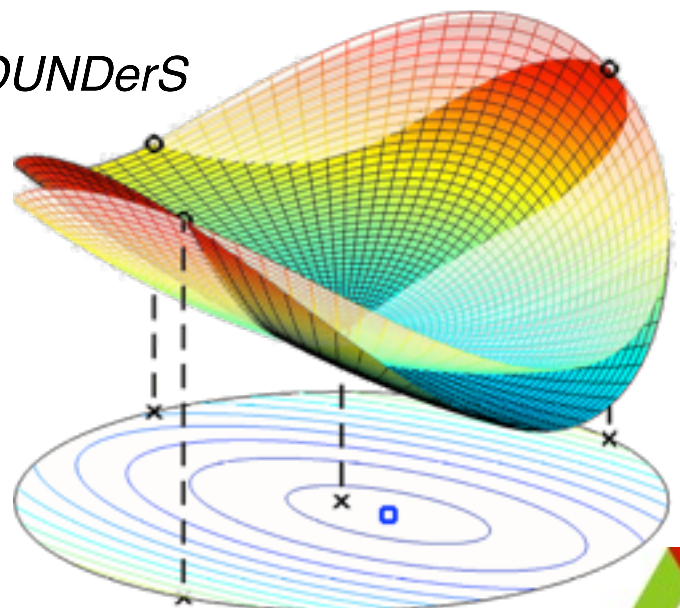

Interaction: NN+3NF(non-local) NNLO cutoff=450 MeV

Optimization: vary all LECs in NN+3NF simultaneously

Design goal: describe binding energies and radii for A=2, 3, 4, p-shell, and sd-shell

$$\min_{\vec{x}} \left[f(\vec{x}) = \sum_{q=1}^{N} \left(\frac{O(\vec{x})_q - O_q^{\exp}}{w_q} \right)^2 \right]$$

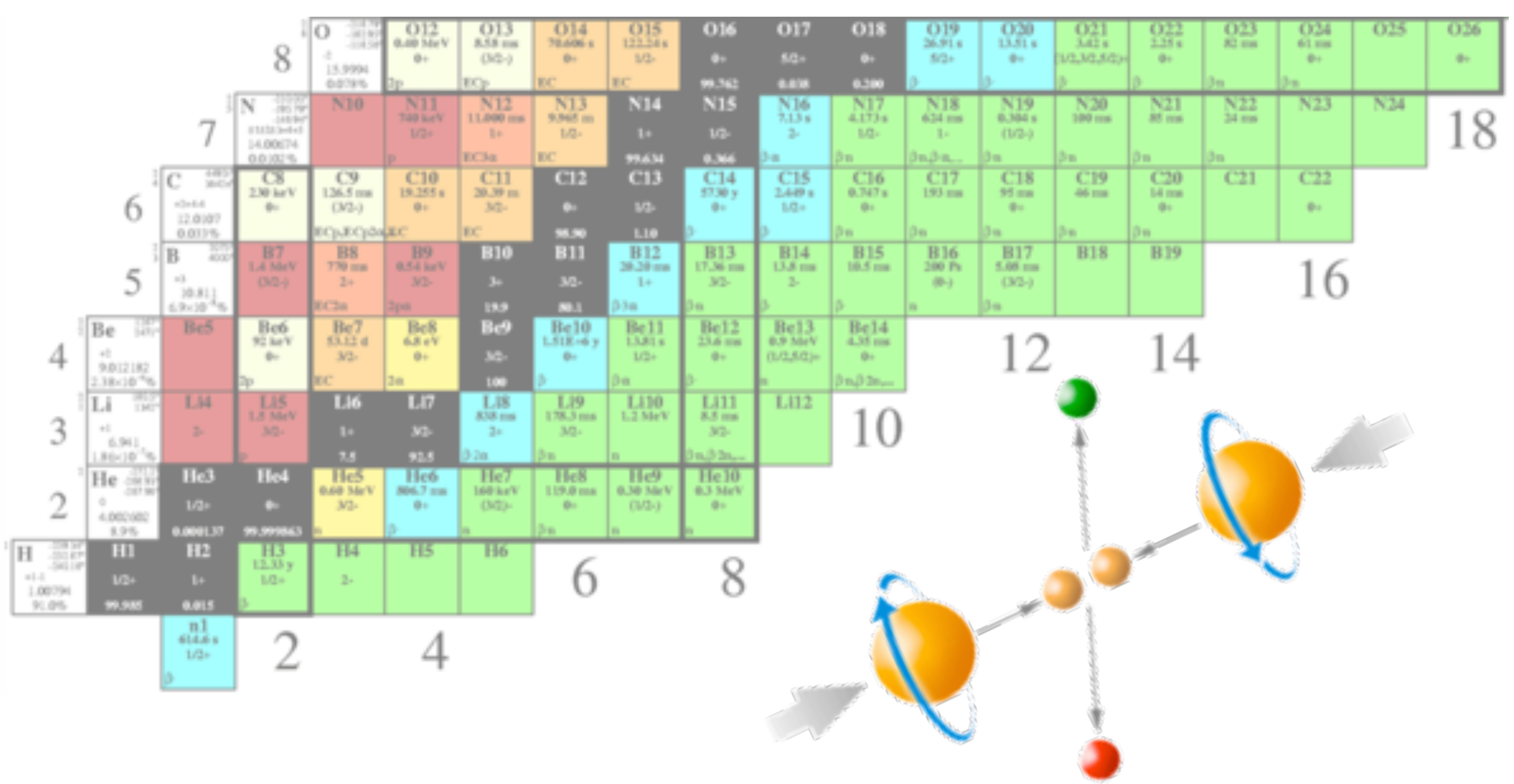

Nucleon-nucleon scattering data up to Tlab=35 MeV

Scattering lengths and effective ranges in the $^1S_0$ channels

NCSM and CCSD(Nmax=8) solutions of binding energies and charge radii for a selected set of light nuclei

in-medium optimization: implementation

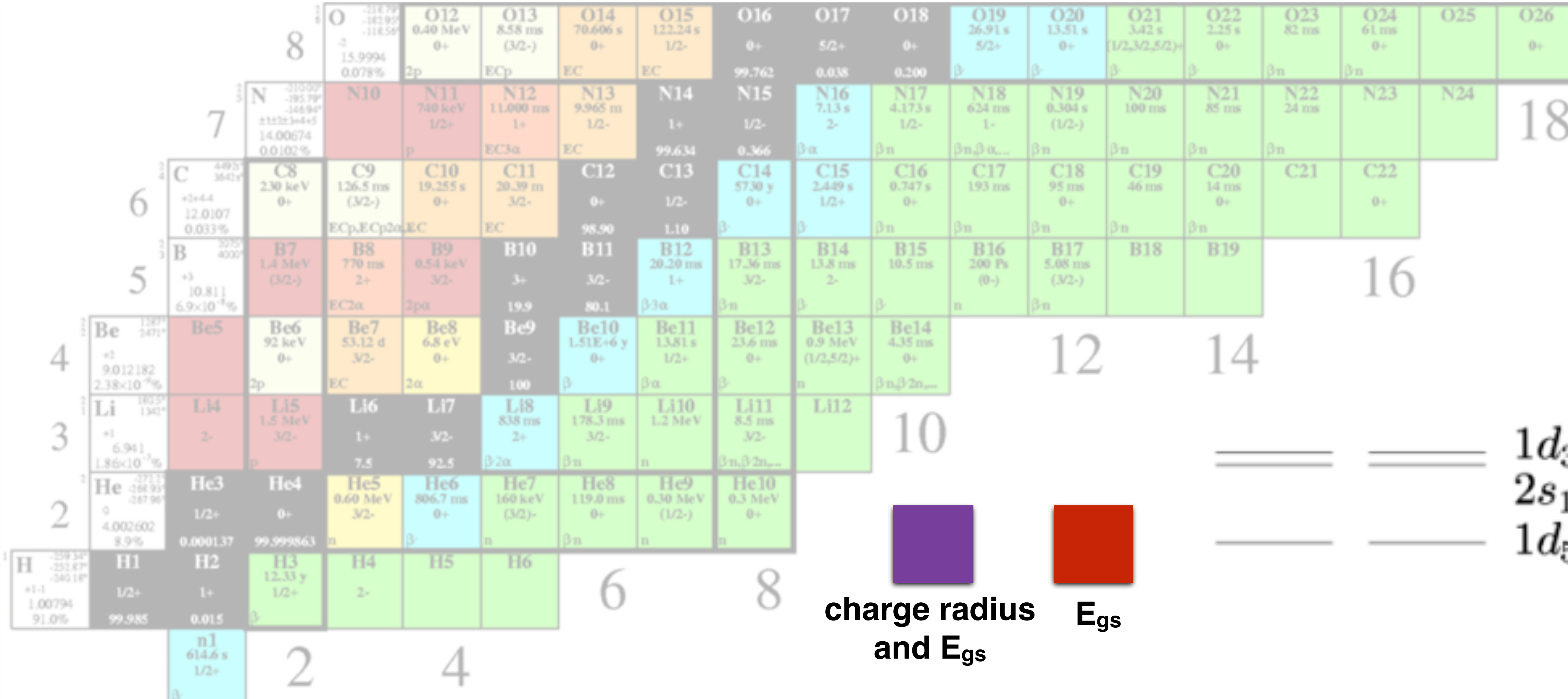

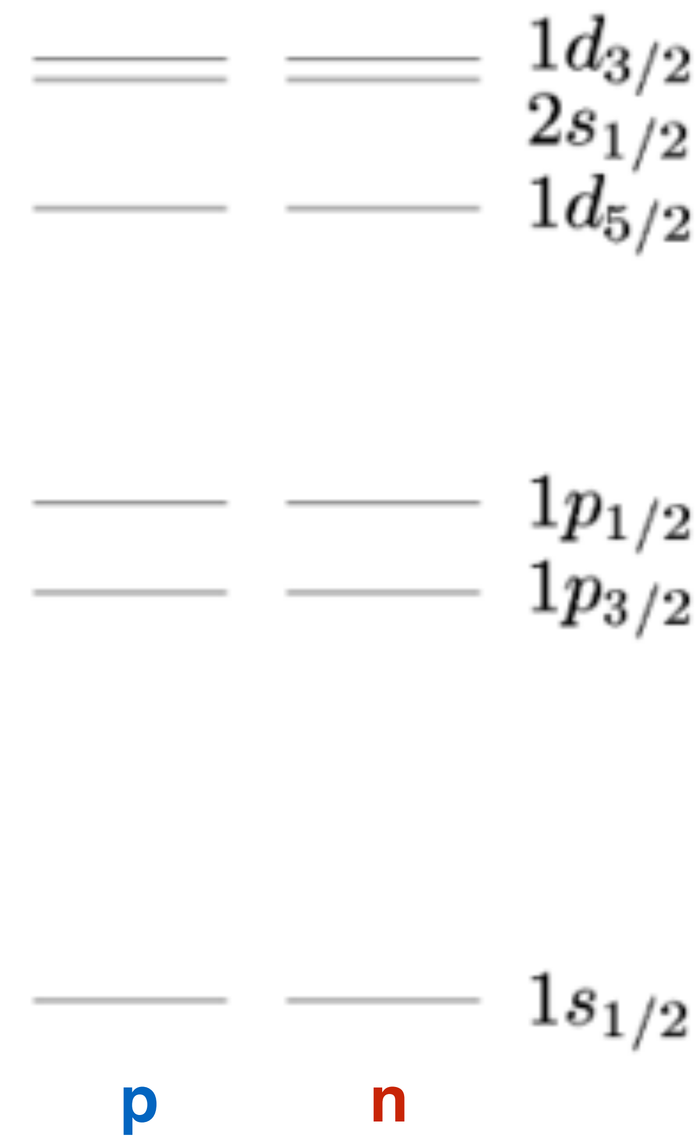

No-Core Shell Model
- Nmax=40/20
- hw=36 MeV

Coupled Cluster
- 3NF in NO2B
- Nmax=8
- hw=22 MeV

for each iteration (3 min) calculate…

…NN-scattering observables and effective ranges

…NCSM results for A=2,3,4 nuclei.

…CCSD results for A=14,16,22,24,25 nuclei.
A nucleus-dependent estimates was employed to account for the effects of a larger model spaces and triples-cluster corrections

in-medium optimization: implementation

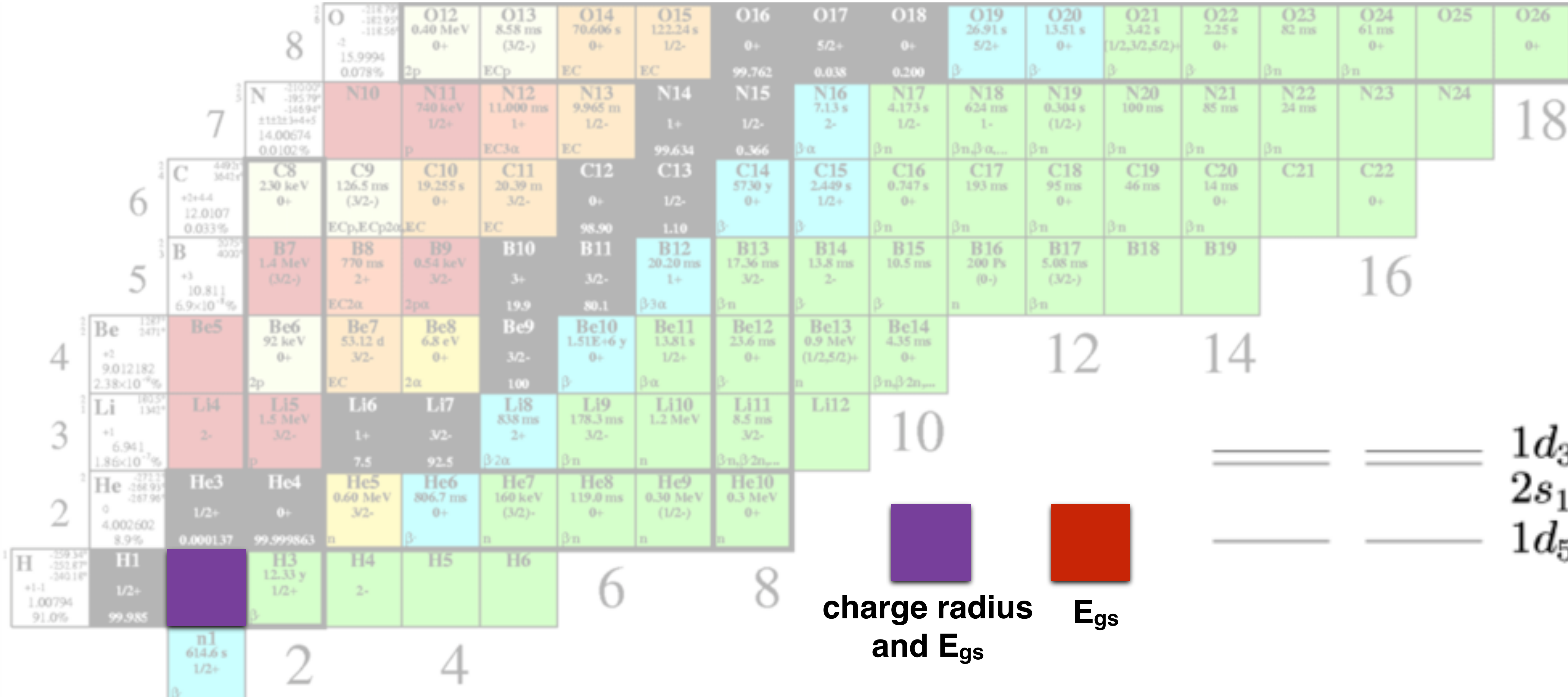

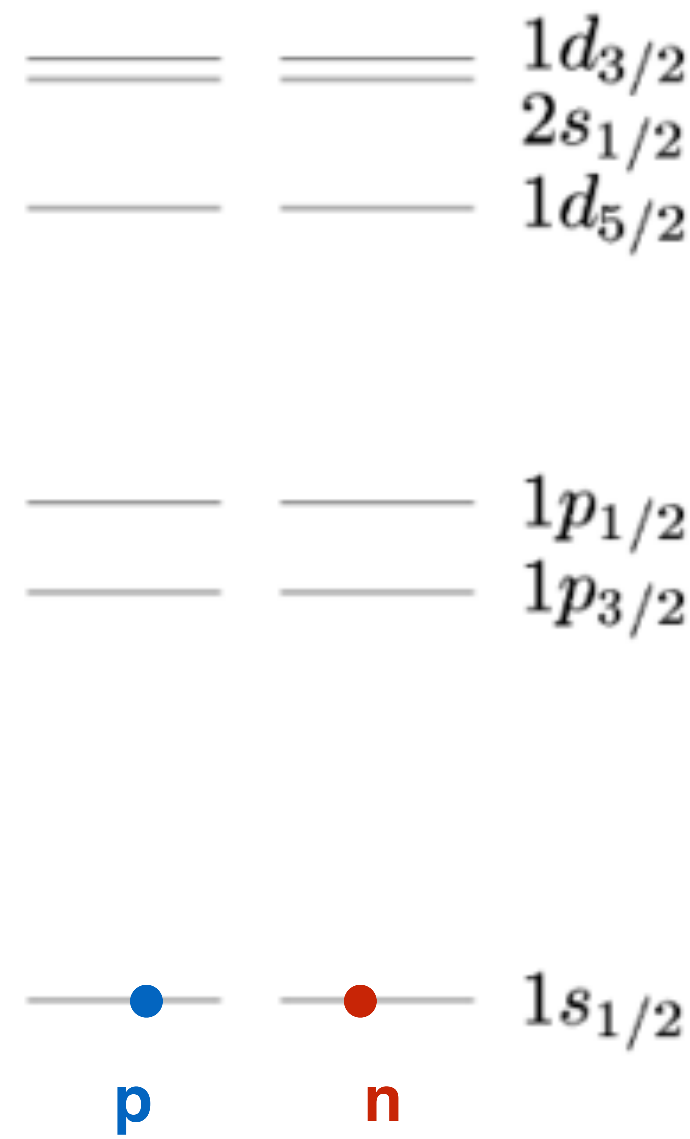

No-Core Shell Model
- Nmax=40/20
- hw=36 MeV

Coupled Cluster
- 3NF in NO2B
- Nmax=8
- hw=22 MeV

for each iteration (3 min) calculate…

…NN-scattering observables and effective ranges

…NCSM results for A=2,3,4 nuclei.

…CCSD results for A=14,16,22,24,25 nuclei.
A nucleus-dependent estimates was employed to account for the effects of a larger model spaces and triples-cluster corrections

in-medium optimization: implementation

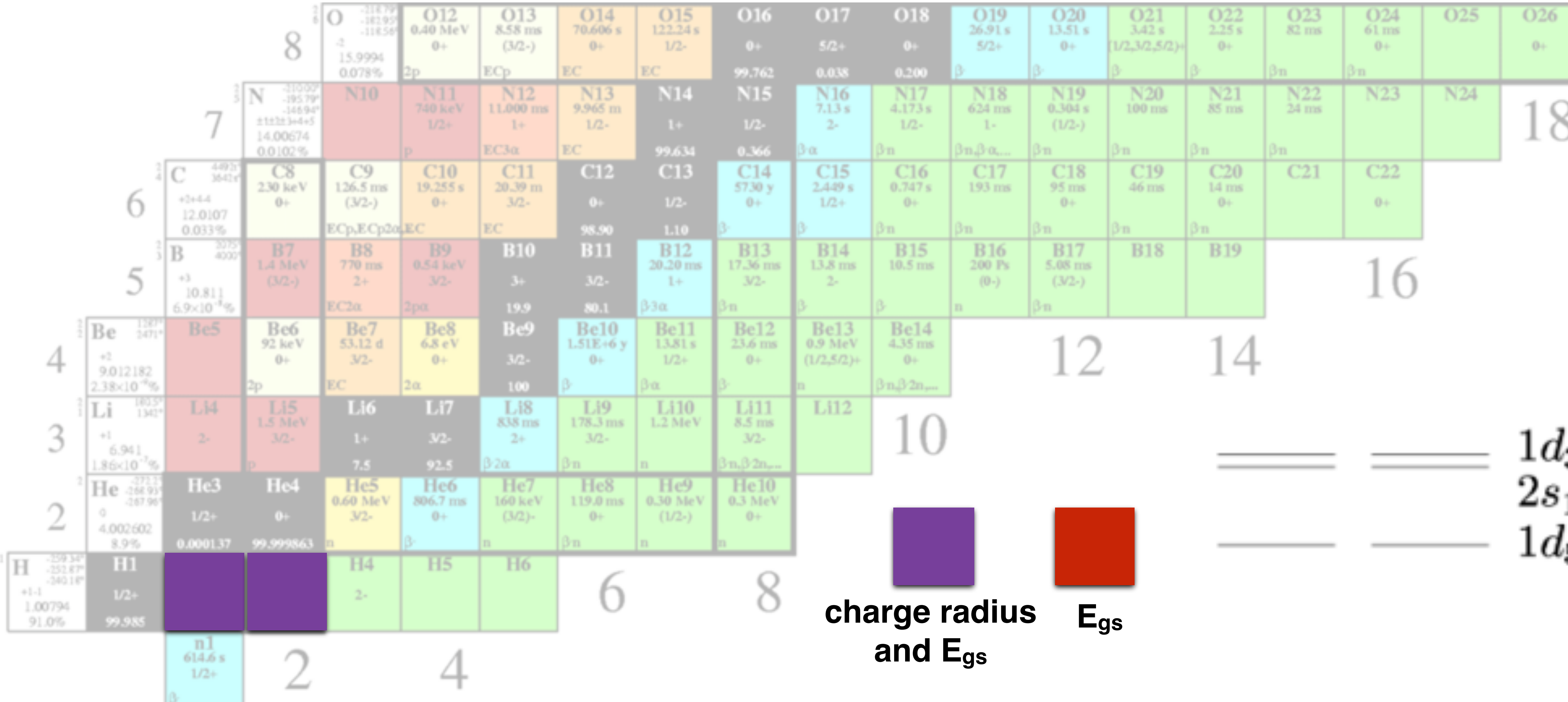

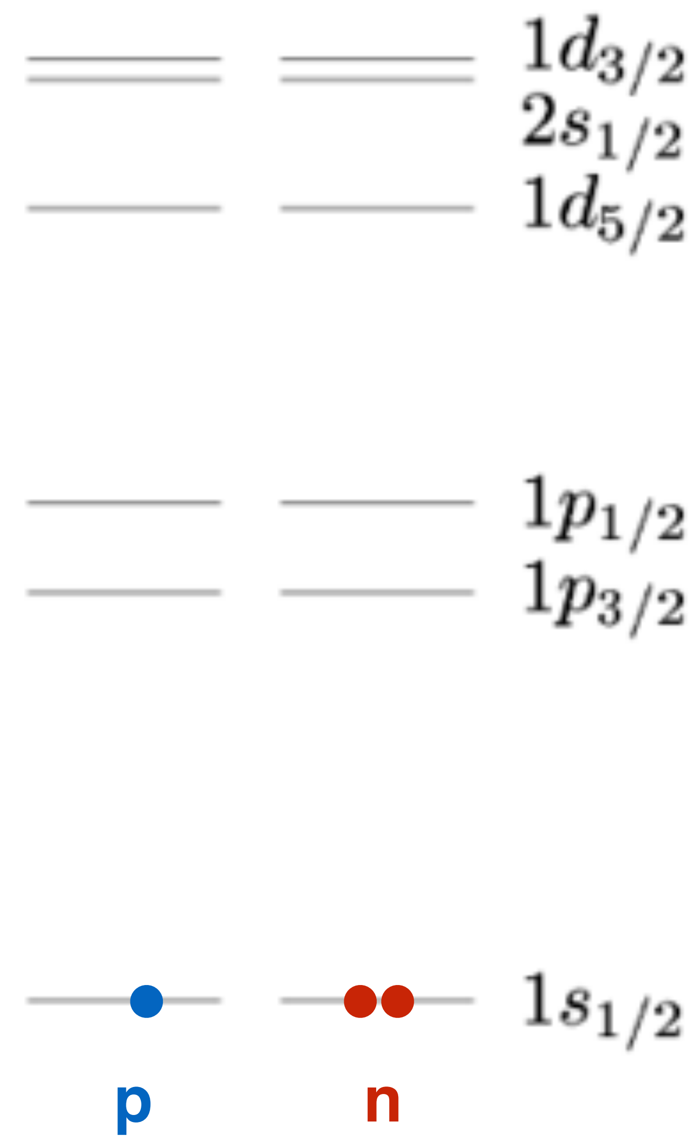

No-Core Shell Model
- Nmax=40/20
- hw=36 MeV

Coupled Cluster
- 3NF in NO2B
- Nmax=8
- hw=22 MeV

for each iteration (3 min) calculate…

…NN-scattering observables and effective ranges

…NCSM results for A=2,3,4 nuclei.

…CCSD results for A=14,16,22,24,25 nuclei.
A nucleus-dependent estimates was employed to account for the effects of a larger model spaces and triples-cluster corrections

in-medium optimization: implementation

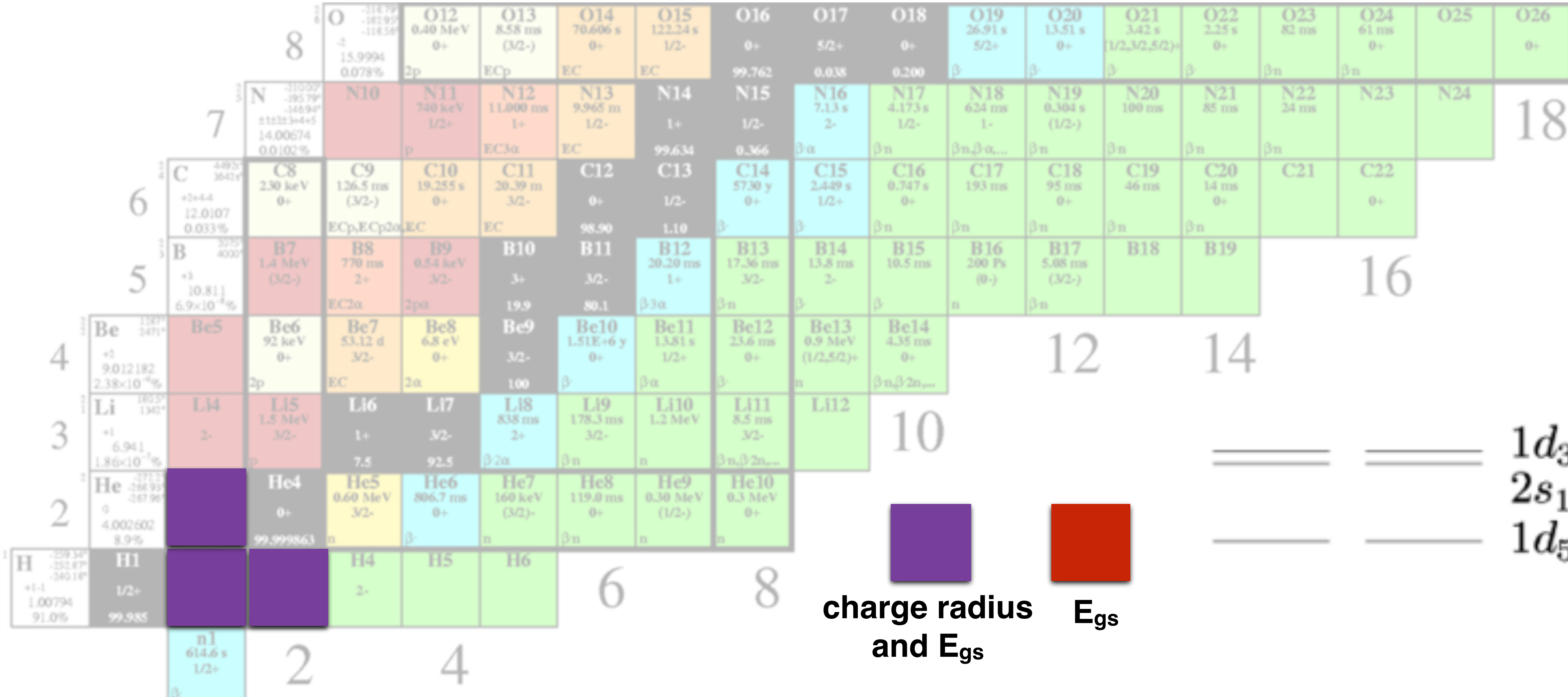

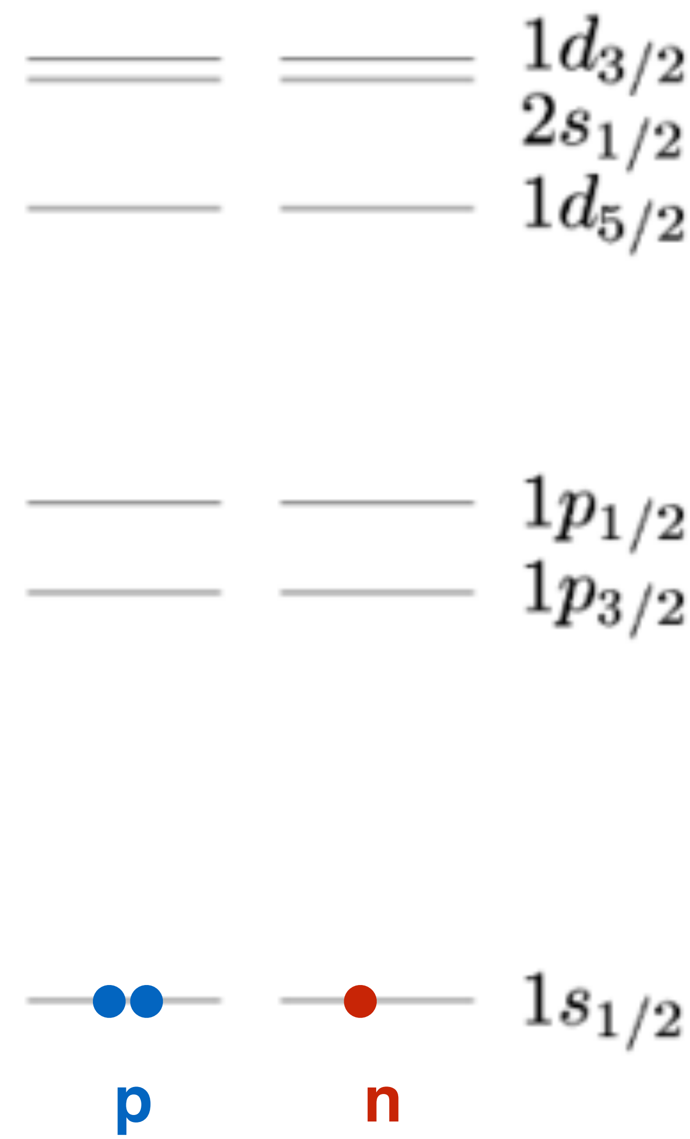

No-Core Shell Model

- Nmax=40/20
- hw=36 MeV

Coupled Cluster

- 3NF in NO2B
- Nmax=8
- hw=22 MeV

for each iteration (3 min) calculate…

…NN-scattering observables and effective ranges

…NCSM results for A=2,3,4 nuclei.

…CCSD results for A=14,16,22,24,25 nuclei.
A nucleus-dependent estimates was employed to account for the effects of a larger model spaces and triples-cluster corrections

in-medium optimization: implementation

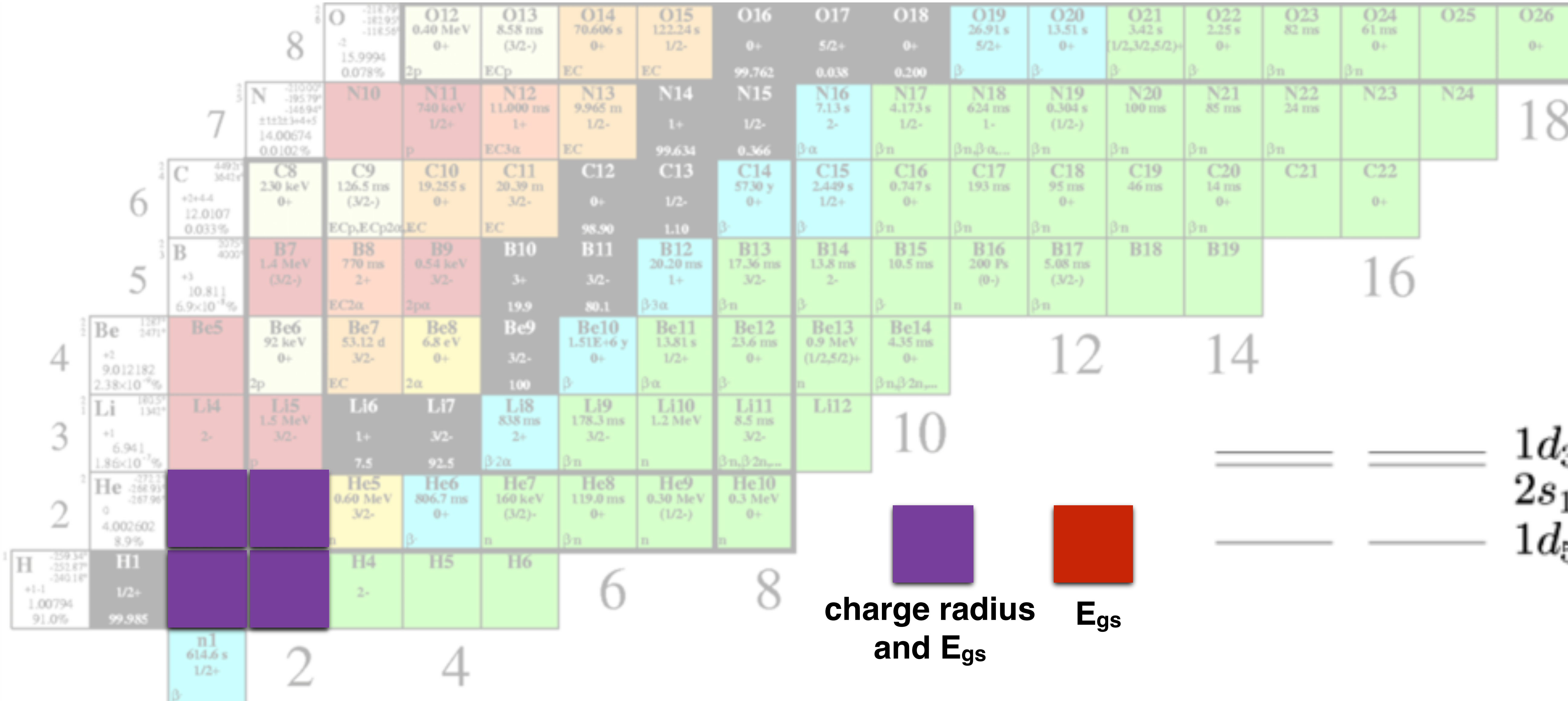

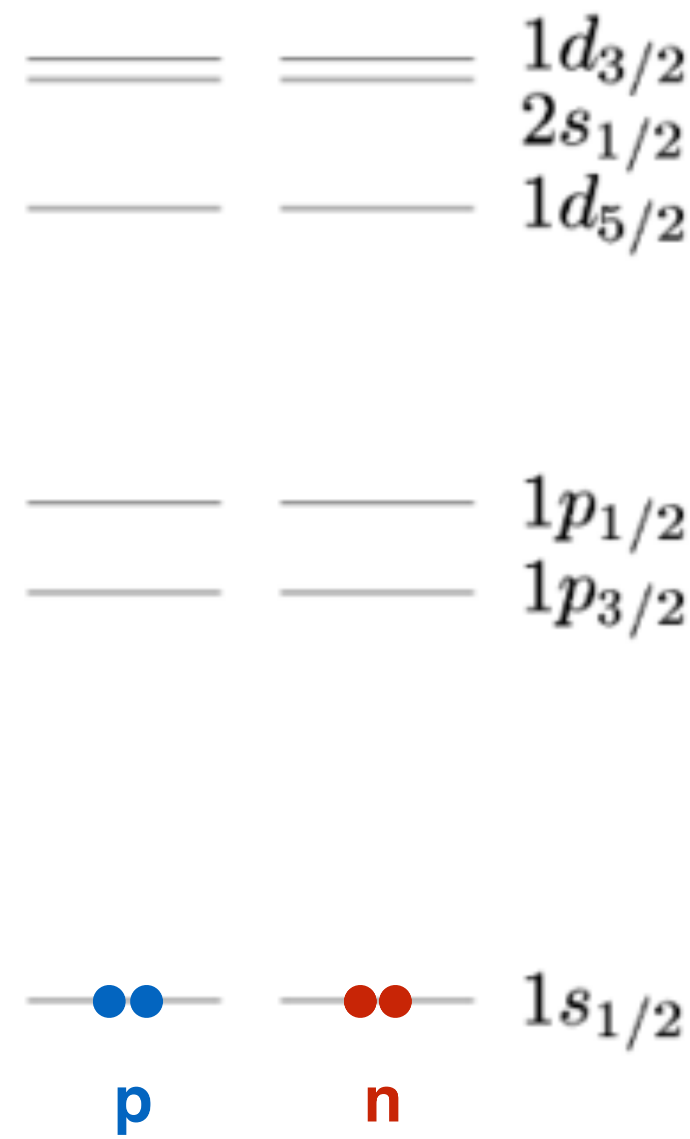

No-Core Shell Model
- Nmax=40/20
- hw=36 MeV

Coupled Cluster
- 3NF in NO2B
- Nmax=8
- hw=22 MeV

for each iteration (3 min) calculate…

…NN-scattering observables and effective ranges

…NCSM results for A=2,3,4 nuclei.

…CCSD results for A=14,16,22,24,25 nuclei.
A nucleus-dependent estimates was employed to account for the effects of a larger model spaces and triples-cluster corrections

in-medium optimization: implementation

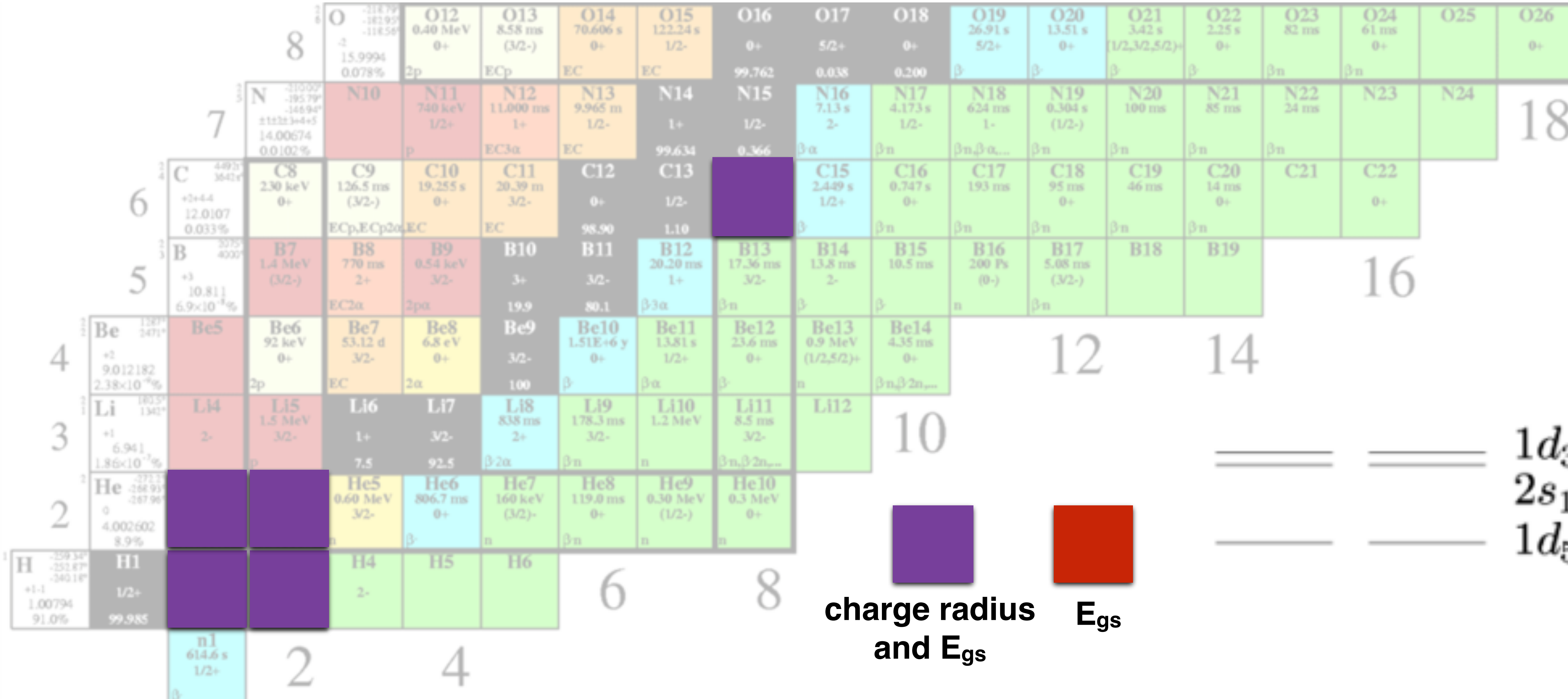

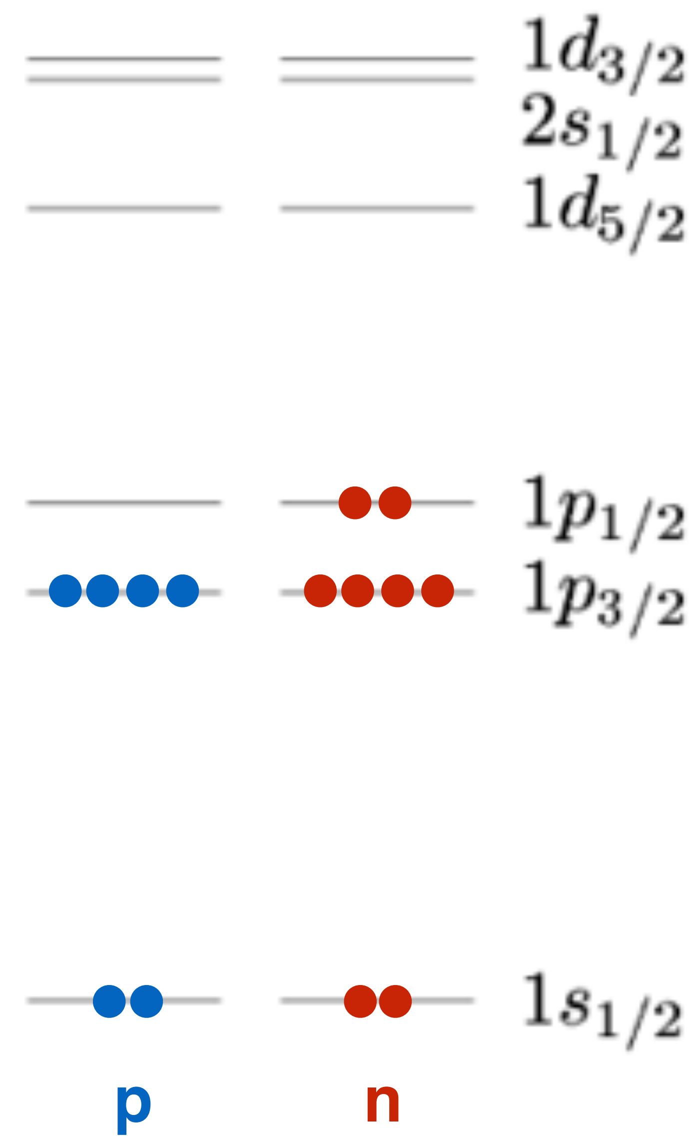

No-Core Shell Model

- Nmax=40/20
- hw=36 MeV

Coupled Cluster

- 3NF in NO2B
- Nmax=8
- hw=22 MeV

for each iteration (3 min) calculate…

…NN-scattering observables and effective ranges

…NCSM results for A=2,3,4 nuclei.

…CCSD results for A=14,16,22,24,25 nuclei.
A nucleus-dependent estimates was employed to account for the effects of a larger model spaces and triples-cluster corrections

in-medium optimization: implementation

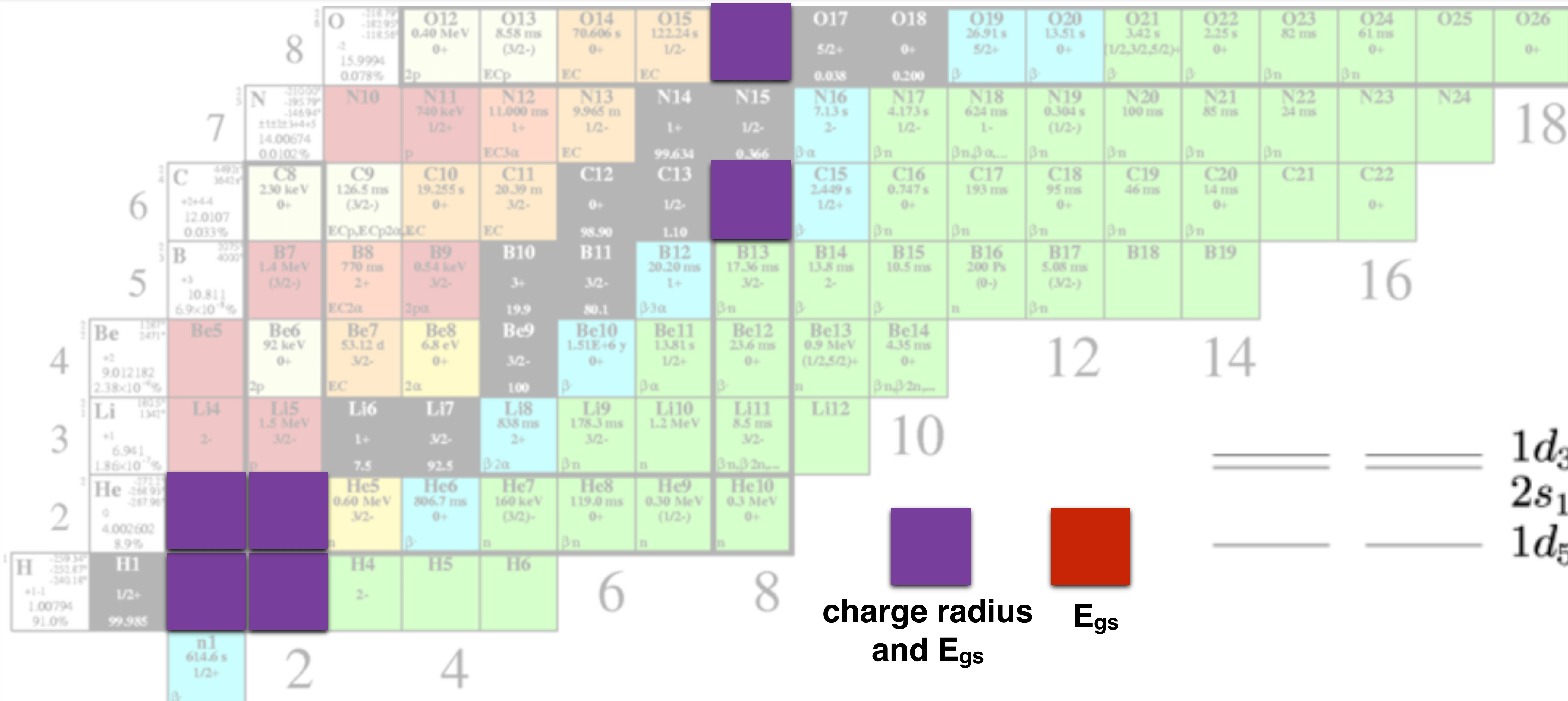

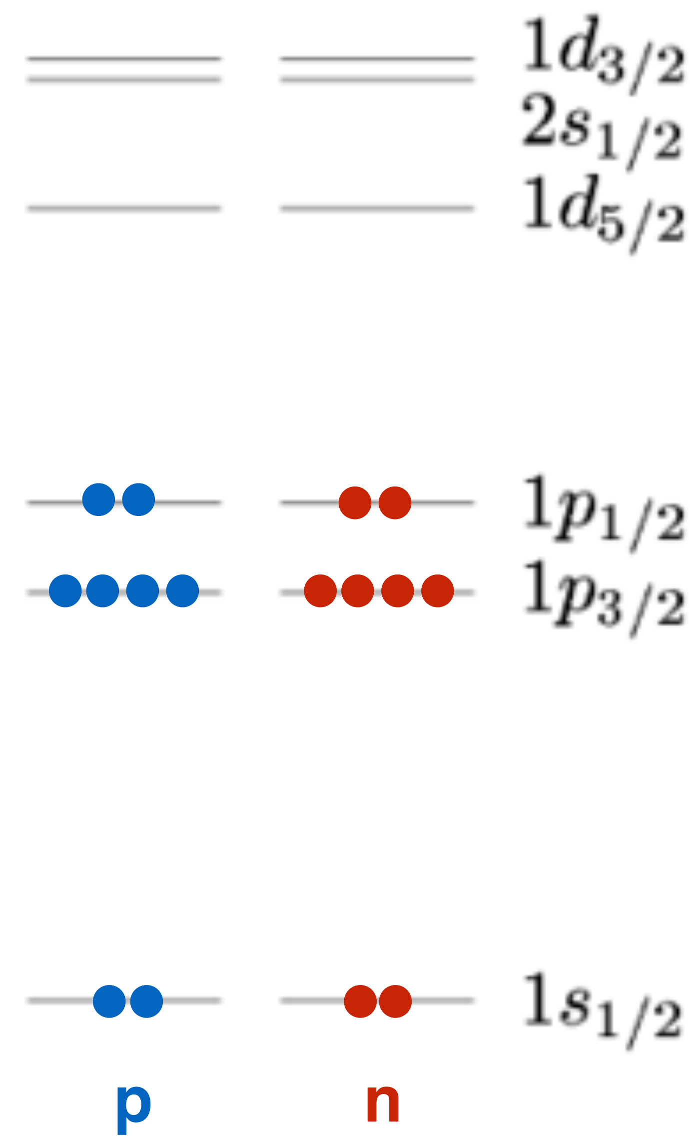

No-Core Shell Model
- Nmax=40/20
- hw=36 MeV

Coupled Cluster
- 3NF in NO2B
- Nmax=8
- hw=22 MeV

for each iteration (3 min) calculate…

…NN-scattering observables and effective ranges

…NCSM results for A=2,3,4 nuclei.

…CCSD results for A=14,16,22,24,25 nuclei.
A nucleus-dependent estimates was employed to account for the effects of a larger model spaces and triples-cluster corrections

in-medium optimization: implementation

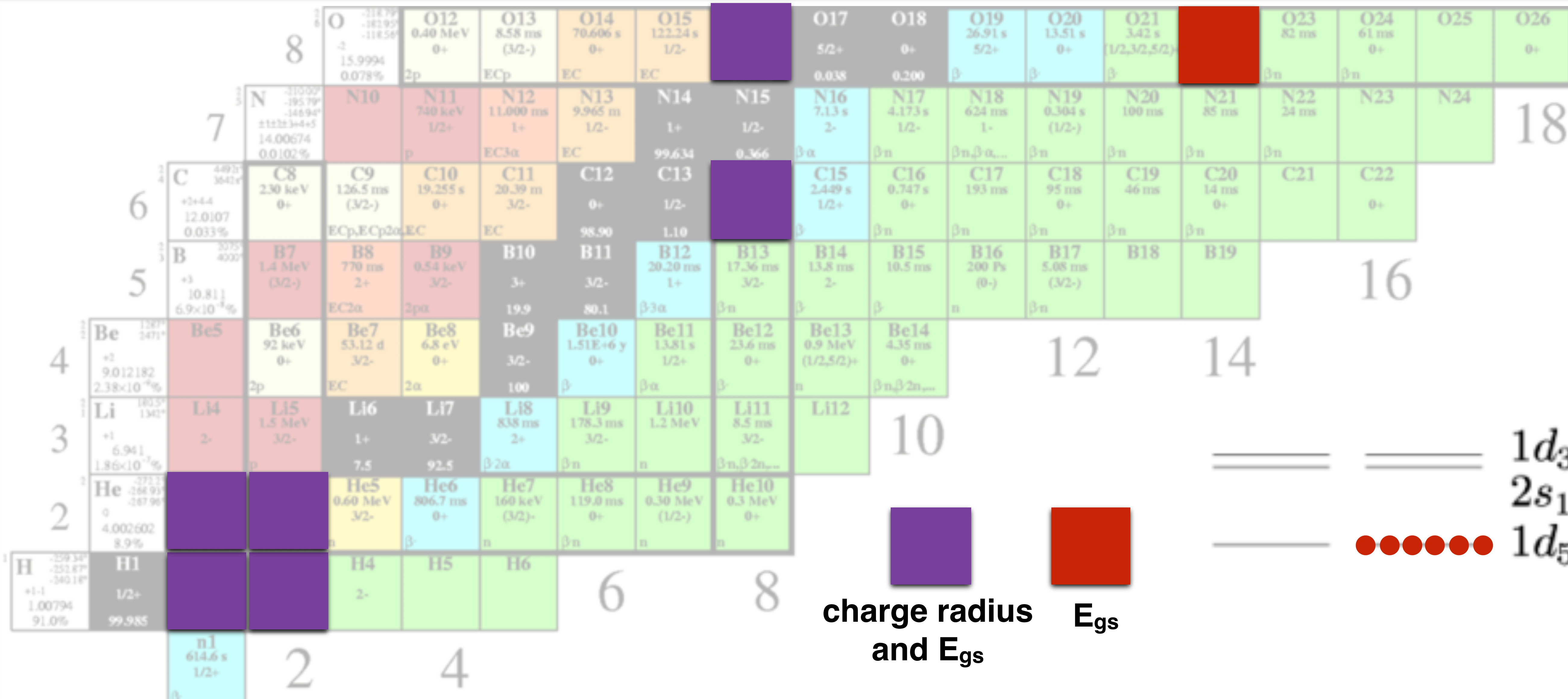

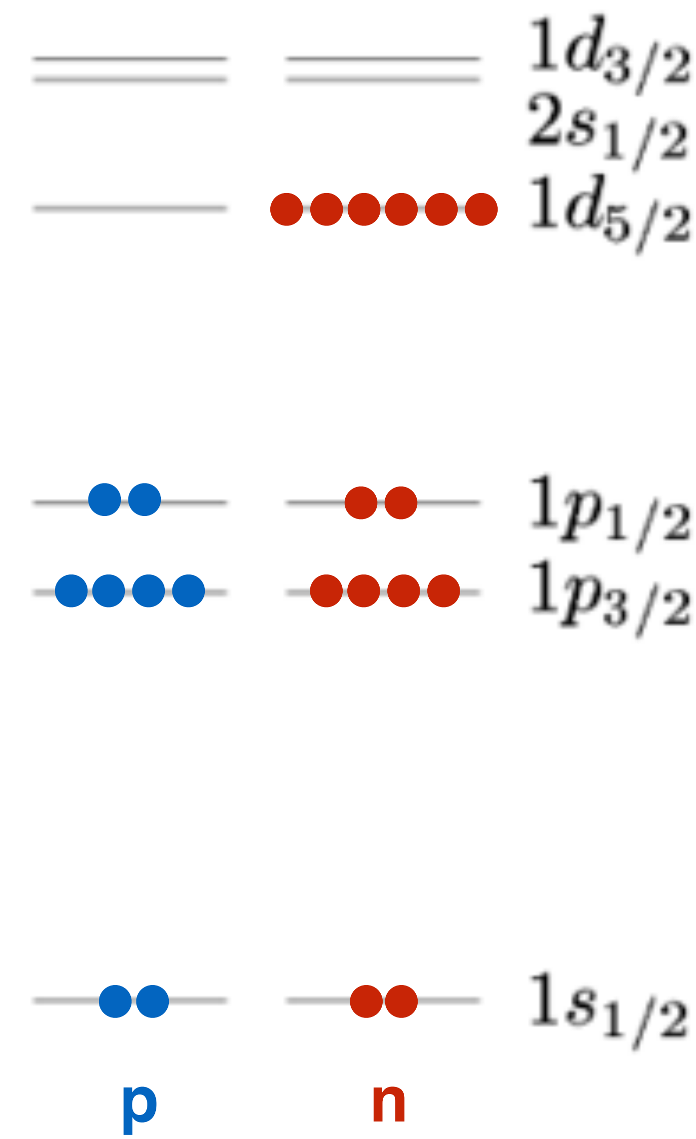

No-Core Shell Model
- Nmax=40/20
- hw=36 MeV

Coupled Cluster
- 3NF in NO2B
- Nmax=8
- hw=22 MeV

for each iteration (3 min) calculate…

…NN-scattering observables and effective ranges

…NCSM results for A=2,3,4 nuclei.

…CCSD results for A=14,16,22,24,25 nuclei.
A nucleus-dependent estimates was employed to account for the effects of a larger model spaces and triples-cluster corrections

in-medium optimization: implementation

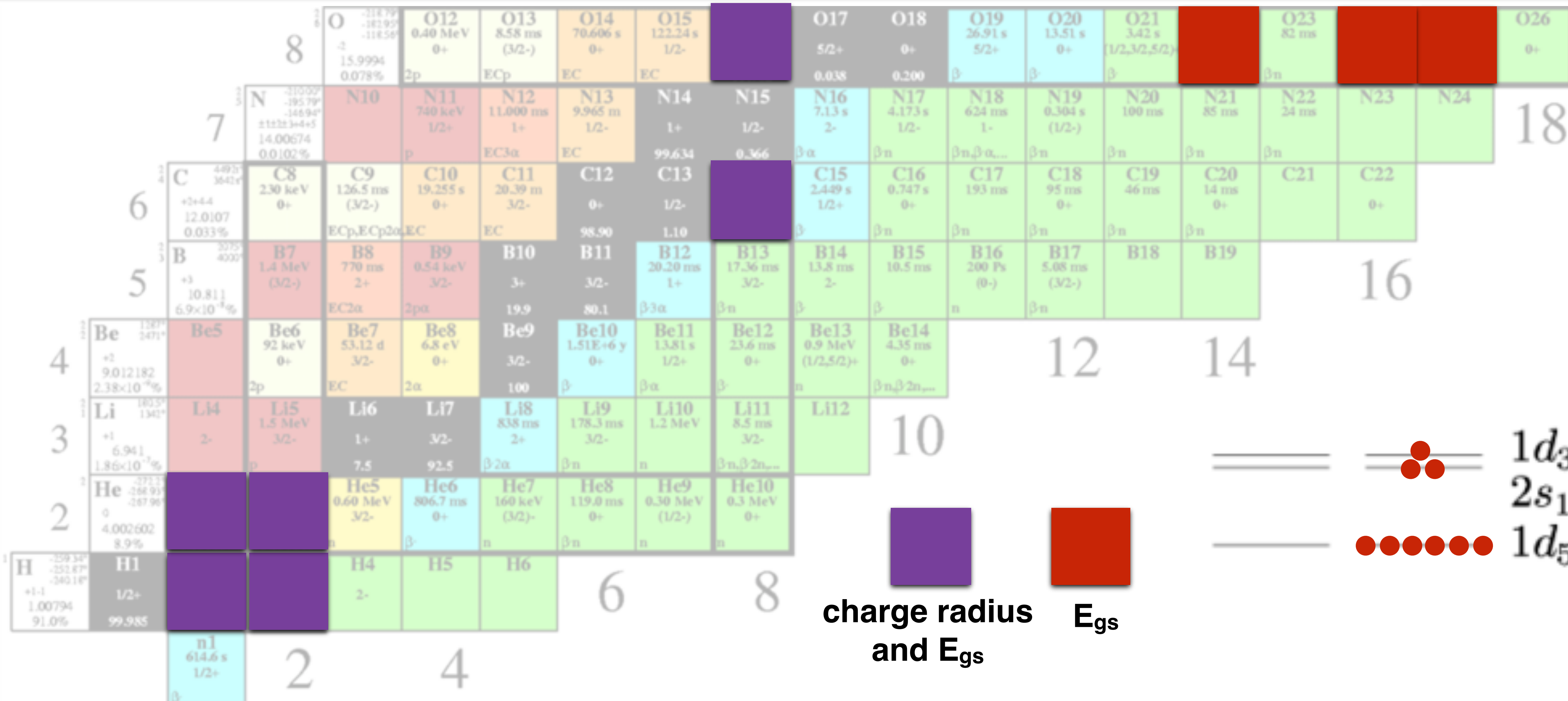

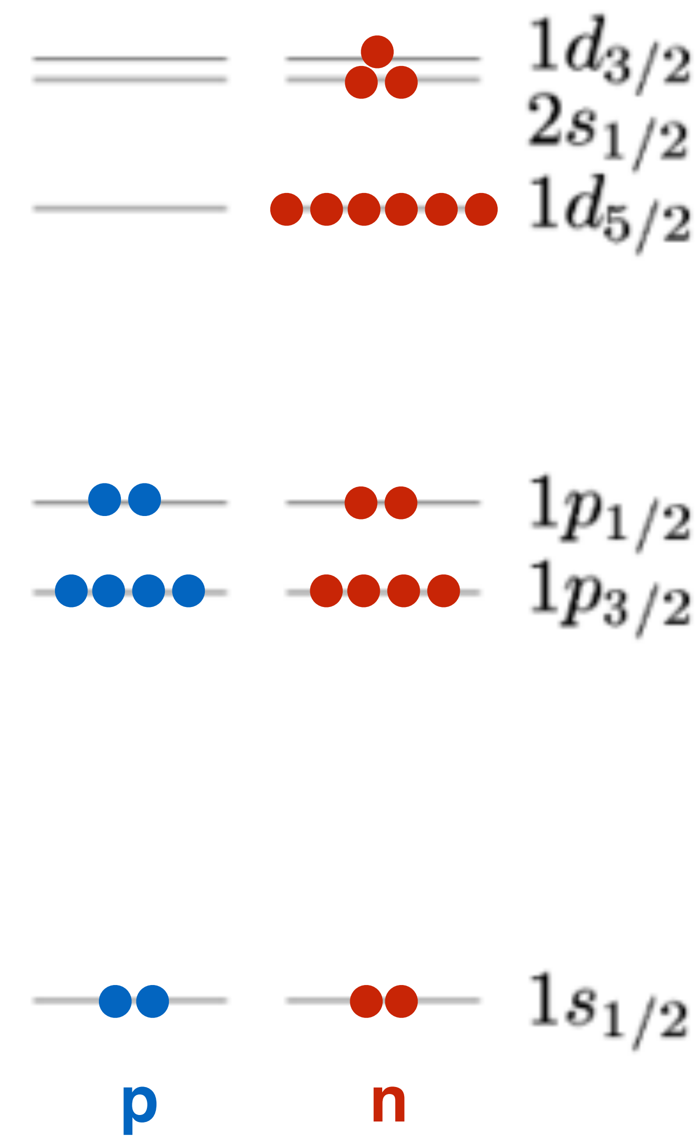

No-Core Shell Model

- Nmax=40/20
- hw=36 MeV

Coupled Cluster

- 3NF in NO2B
- Nmax=8
- hw=22 MeV

for each iteration (3 min) calculate…

…NN-scattering observables and effective ranges

…NCSM results for A=2,3,4 nuclei.

…CCSD results for A=14,16,22,24,25 nuclei.
A nucleus-dependent estimates was employed to account for the effects of a larger model spaces and triples-cluster corrections

in-medium optimization: implementation

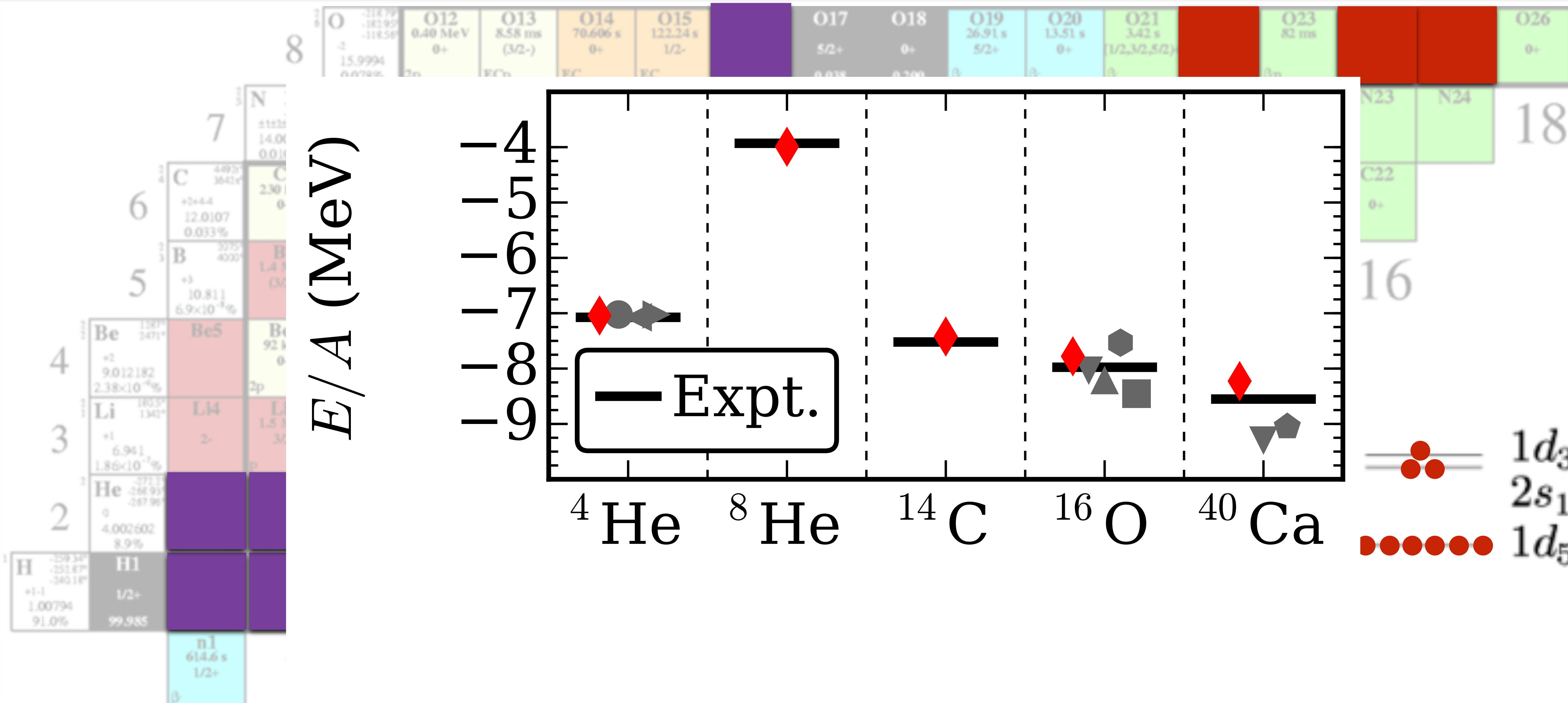

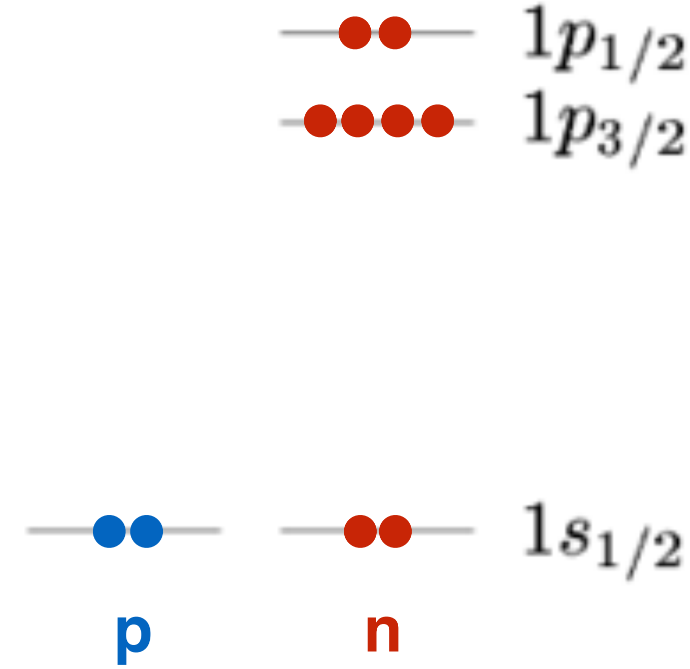

No-Core Shell M

- Nmax=40/2
- hw=36 MeV

Coupled Cluster

- 3NF in NO2B
- Nmax=8
- hw=22 MeV

A nucleus-dependent estimates was employed to account for the effects of a larger model spaces and triples-cluster corrections

in-medium optimization: implementation

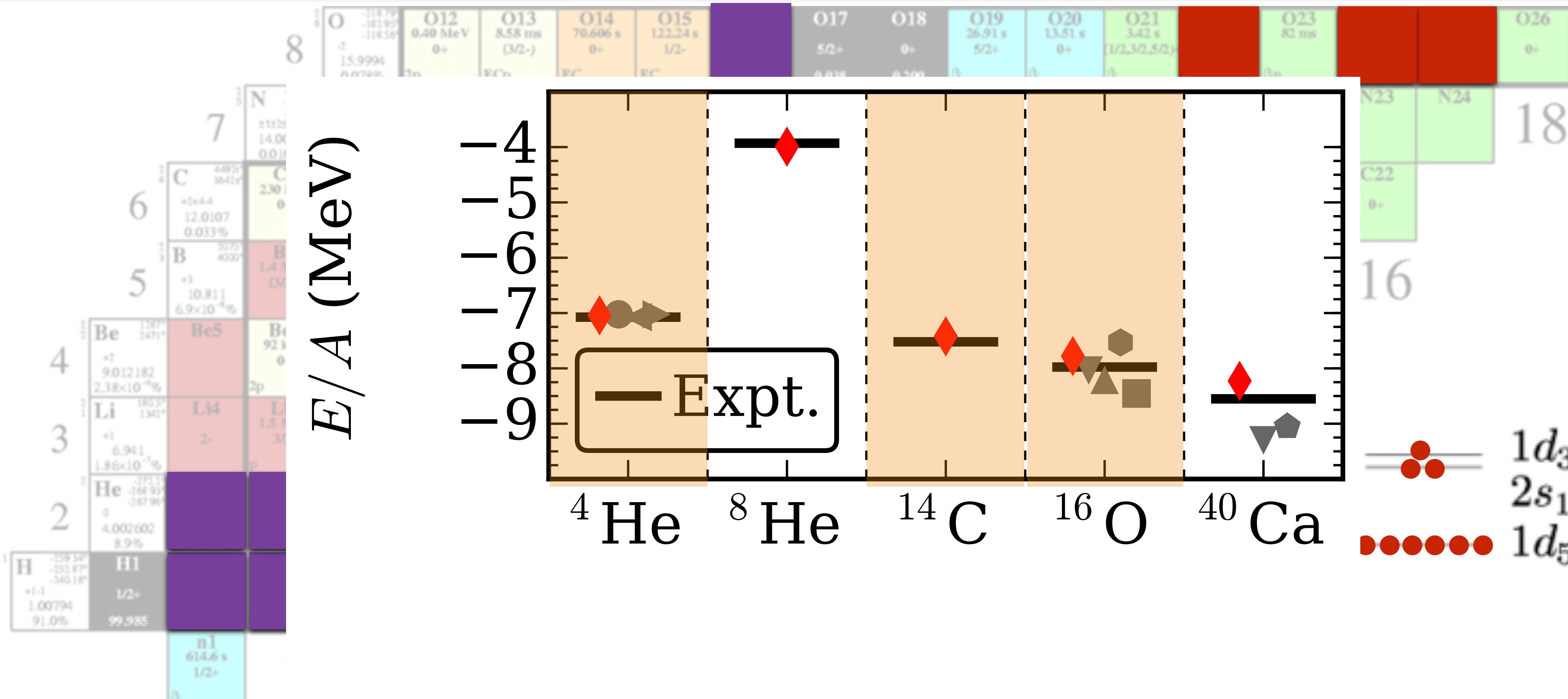

No-Core Shell M

- Nmax=40/2
- hw=36 MeV

Coupled Cluster

- 3NF in NO2B
- Nmax=8
- hw=22 MeV

A nucleus-dependent estimates was employed to account for the effects of a larger model spaces and triples-cluster corrections

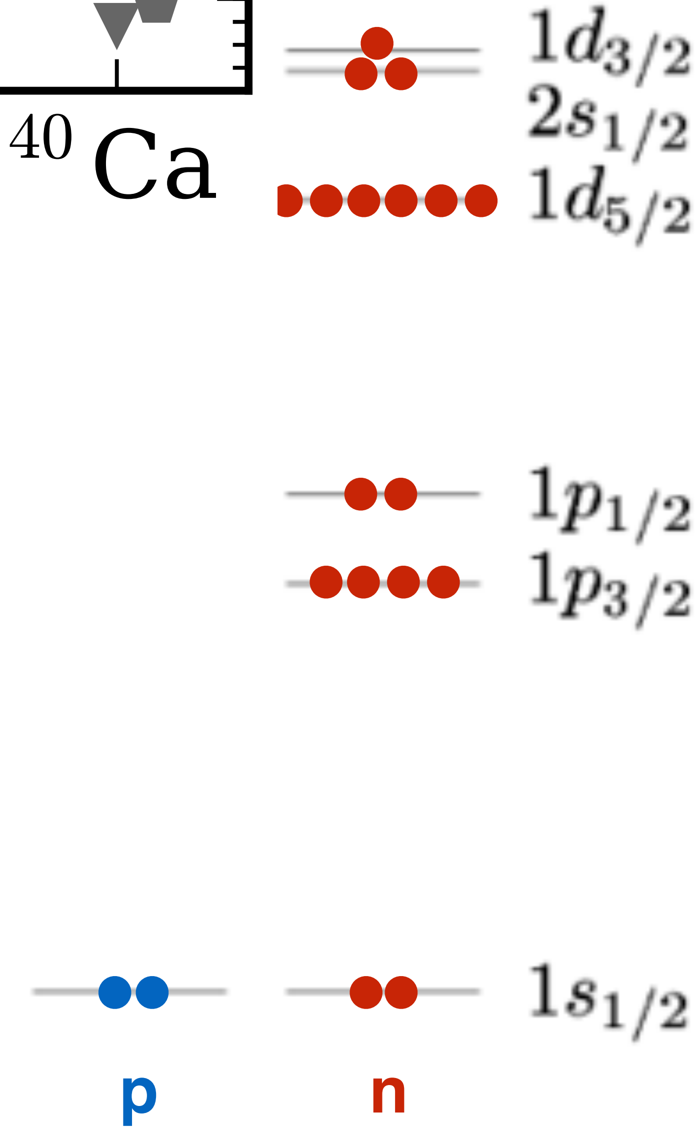

in-medium optimization: implementation

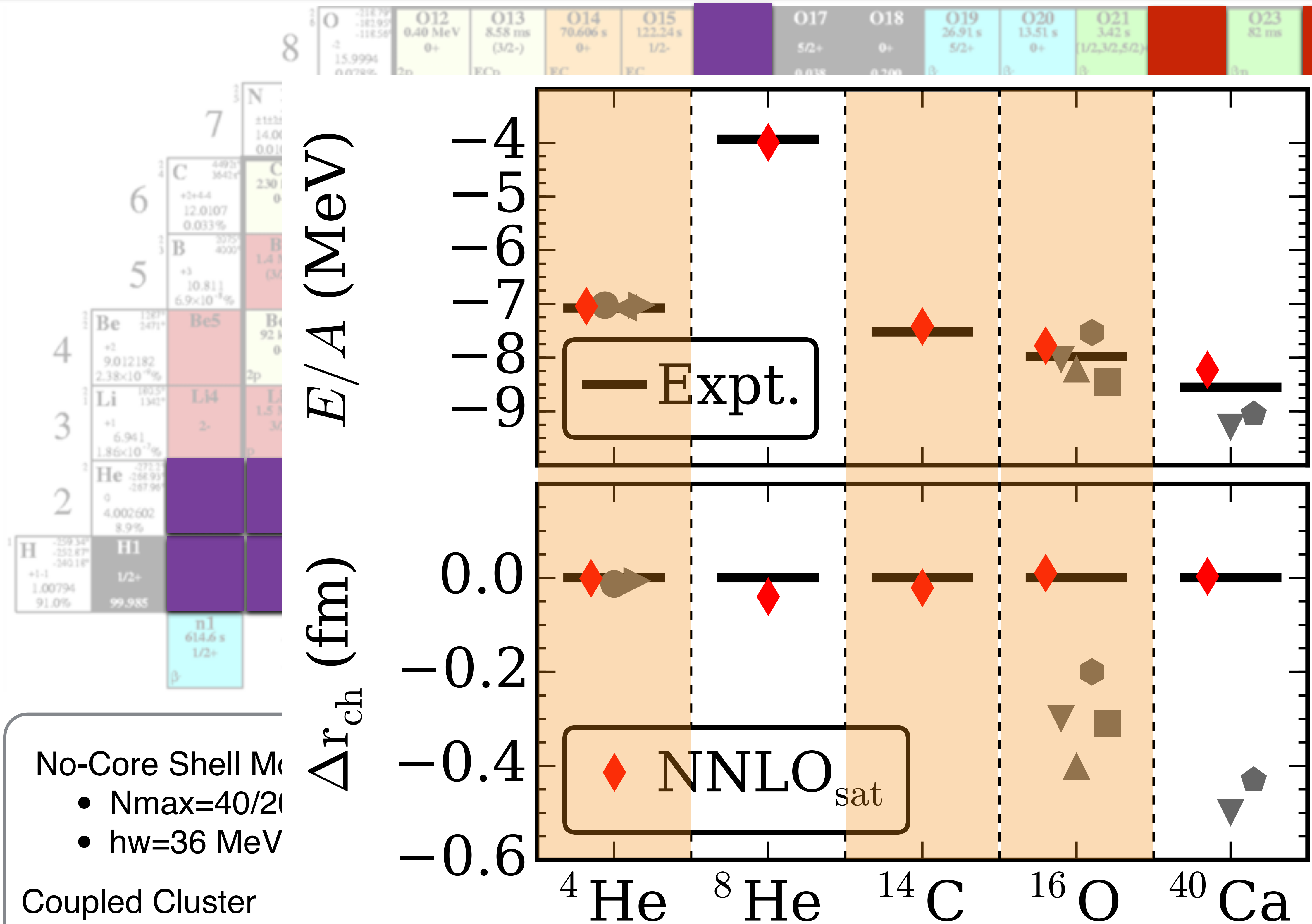

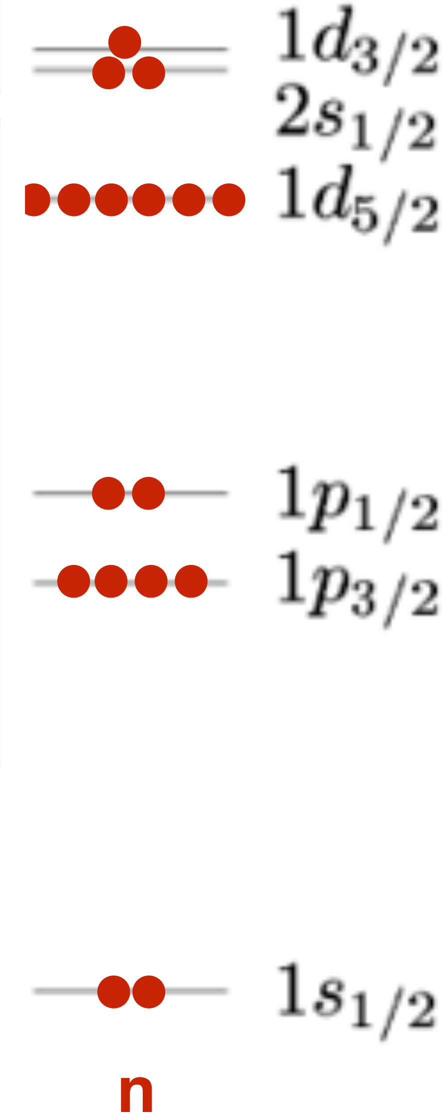

No-Core Shell M
- Nmax=40/2
- hw=36 MeV

Coupled Cluster
- 3NF in NO2B
- Nmax=8
- hw=22 MeV

A nucleus-dependent estimates was employed to account for the effects of a larger model spaces and triples-cluster corrections

NNLO$_{sat}$ and the reproduction of input data

NCSM Energies and charge radii with NNLOsat

Observable	Theory	Experiment	D/Exp (%)
$E_{gs}(^2H)$	-2.224574	2.224575(9) MeV	0.0
$r_{pt-p}(^2H)$	1.978	1.97535(85) fm	0.1
$Q_D(^2H)$	0.270	0.2859(3) fm^2	5.6
$P_D(^2H)$	3.46%	—	—
$E_{gs}(^3H)$	-8.52	-8.482 MeV	0.4
$r_{ch}(^3H)$	1.78	1.7591(363) fm	1.1
$E_{gs}(^3He)$	-7.76	-7.718 MeV	0.5
$r_{ch}(^3He)$	1.99	1.9661(30) fm	1.2
$E_{gs}(^4He)$	-28.43	-28.296 MeV	0.5
$r_{ch}(^4He)$	1.70	1.6755(28) fm	1.5

CCSD Energies and charge radii with NNLOsat

Observable	Theory	Experiment	D/Exp (%)
$E_{gs}(^{14}C)$	103.6	105.285 MeV	1.6
$r_{ch}(^{14}C)$	2.48	2.5025(87) fm	0.9
$E_{gs}(^{16}O)$	124.4	127.619 MeV	2.5
$r_{ch}(^{16}O)$	2.71	2.6991(52) fm	0.4
$E_{gs}(^{22}O)$	160.8	162.028(57) MeV	0.8
$E_{gs}(^{24}O)$	168.1	168.96(12) MeV	0.5
$E_{gs}(^{25}O)$	167.4	168.18(10) MeV	0.5

$^1S_0$ effective range expansion

Observable	Theory	Experiment	D/Exp (%)
a_{nn}	-18.93	-18.9(4) fm	0.2
r_{nn}	2.911	2.75(11) fm	5.9
a_{np}	-23.728	-23.740(20) fm	0.0
r_{np}	2.798	2.77(5) fm	1.0
a_{pp}	-7.8258	-7.8196(26) fm	0.0
r_{pp}	2.855	2.790(14) fm	2.3

$$\langle r^2_{\rm ch}\rangle = \langle r^2_{\rm pp}\rangle + \langle R^2_{\rm p}\rangle + \frac{N}{Z}\langle R^2_{\rm n}\rangle + \frac{3\hbar^2}{4m_p^2c^2}$$

R_p=0.8775 fm

$(R_n)^2$=-0.1149 fm^2

Darwin-Foldy=0.033 fm^2

$NNLO_{sat}$ and the reproduction of input data

NCSM Energies and charge radii with NNLOsat

Observable	Theory	Experiment	D/Exp (%)
$E_{gs}(^2H)$	-2.224574	2.224575(9) MeV	0.0
$r_{pt-p}(^2H)$	1.978	1.97535(85) fm	0.1
$Q_D(^2H)$	0.270	0.2859(3) fm^2	5.6
$P_D(^2H)$	3.46%	—	—
$E_{gs}(^3H)$	-8.52	-8.482 MeV	0.4
$r_{ch}(^3H)$	1.78	1.7591(363) fm	1.1
$E_{gs}(^3He)$	-7.76	-7.718 MeV	[illegible]
$r_{ch}(^3He)$	1.99	1.9661(30) f[illegible]	[illegible]
$E_{gs}(^4He)$	-28.43	-28.296 Me[illegible]	[illegible]
$r_{ch}(^4He)$	1.70	1.6755(28) f[illegible]	[illegible]

CCSD Energies and charge radii with NNLOsat

Observable	Theory	Experiment	D/Exp (%)
$E_{gs}(^{14}C)$	103.6	105.285 MeV	1.6
$r_{ch}(^{14}C)$	2.48	2.5025(87) fm	0.9
$E_{gs}(^{16}O)$	124.4	127.619 MeV	2.5
$r_{ch}(^{16}O)$	2.71	2.6991(52) fm	0.4
$E_{gs}(^{22}O)$	160.8	162.028(57) MeV	0.8
$E_{gs}(^{24}O)$	168.1	168.96(12) MeV	0.5
[illegible]	[illegible]	[illegible]	[illegible]

$^1S_0$ effective range expansion

Observable	Theory	Experimen[illegible]	[illegible]
a_{nn}	-18.93	-18.9(4) fm	[illegible]
r_{nn}	2.911	2.75(11) fm	5.9
a_{np}	-23.728	-23.740(20) fm	0.0
r_{np}	2.798	2.77(5) fm	1.0
a_{pp}	-7.8258	-7.8196(26) fm	0.0
r_{pp}	2.855	2.790(14) fm	2.3

$NNLO_{sat}$
*reproduces the binding energies and the charge radii of selected psd-shell nuclei to **1%***

$$\langle r^2_{ch}\rangle = \langle r^2_{pp}\rangle + \langle R^2_p\rangle + \frac{N}{Z}\langle R^2_n\rangle + \frac{3\hbar^2}{4m_p^2c^2}$$

R_p=0.8775 fm
$(R_n)^2$=-0.1149 fm^2
Darwin-Foldy=0.033 fm^2

NNLO$_{sat}$ phase shifts and scattering observables

Phase shifts are very reasonable in the low energy range.

For higher energies, NNLO$_{sat}$ falls on the envelope of NNLO

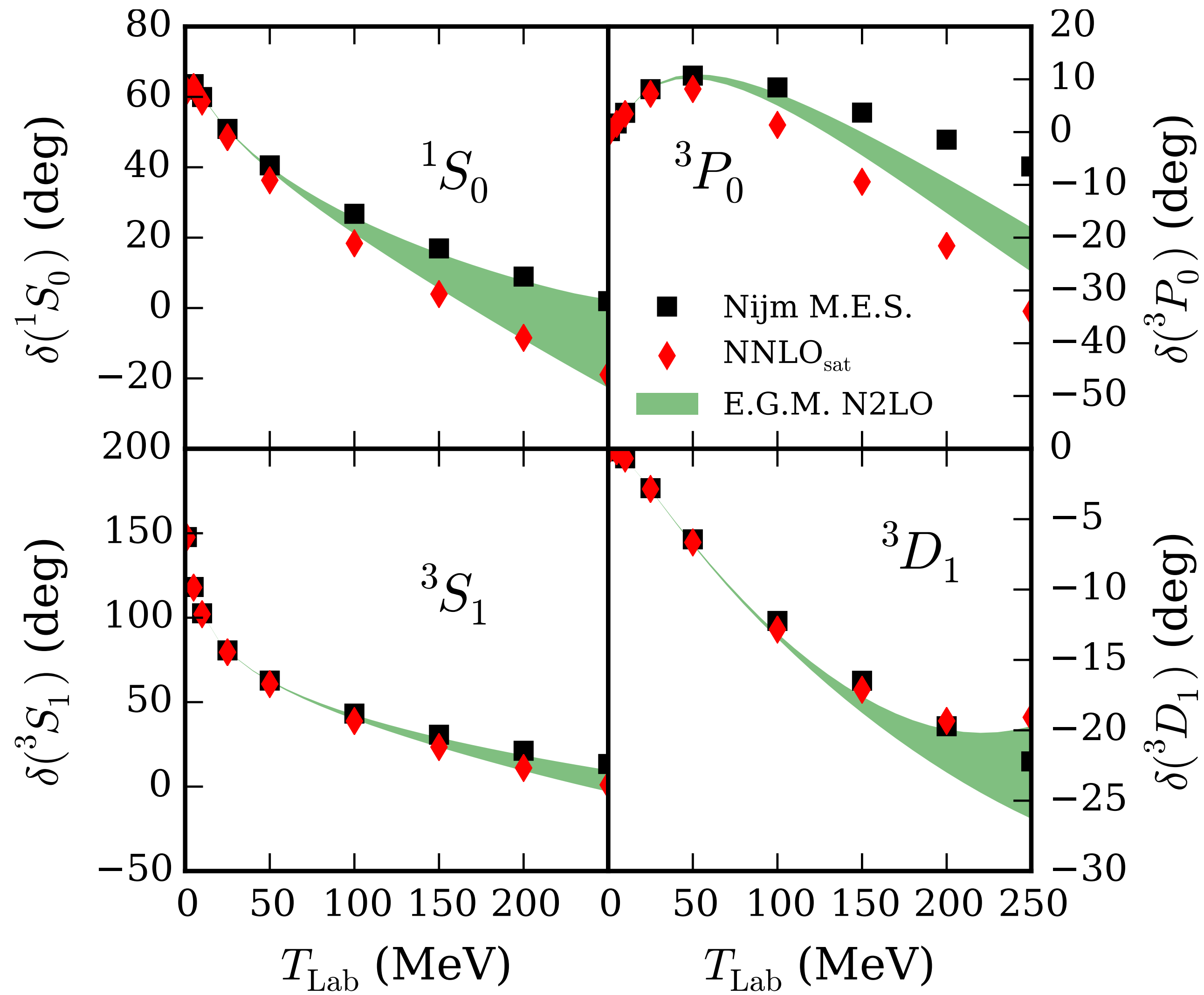

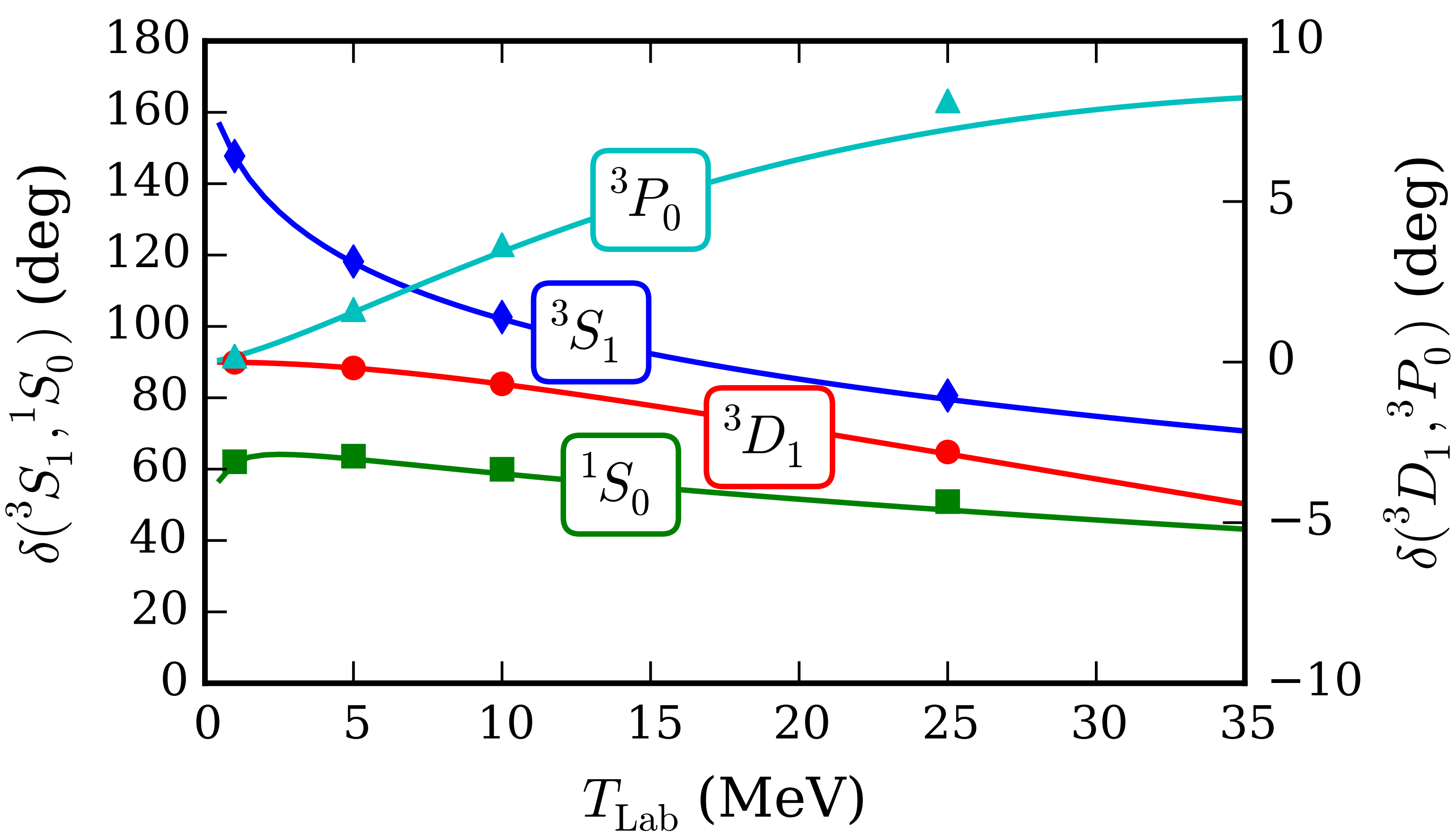

Chi square per datum

T_{Lab}	pp	np
0-35	6	3
35-125	164	7
125-183	118	18
183-290	314	16

Nucleon-nucleon cross sections

Nucleon-nucleon cross sections

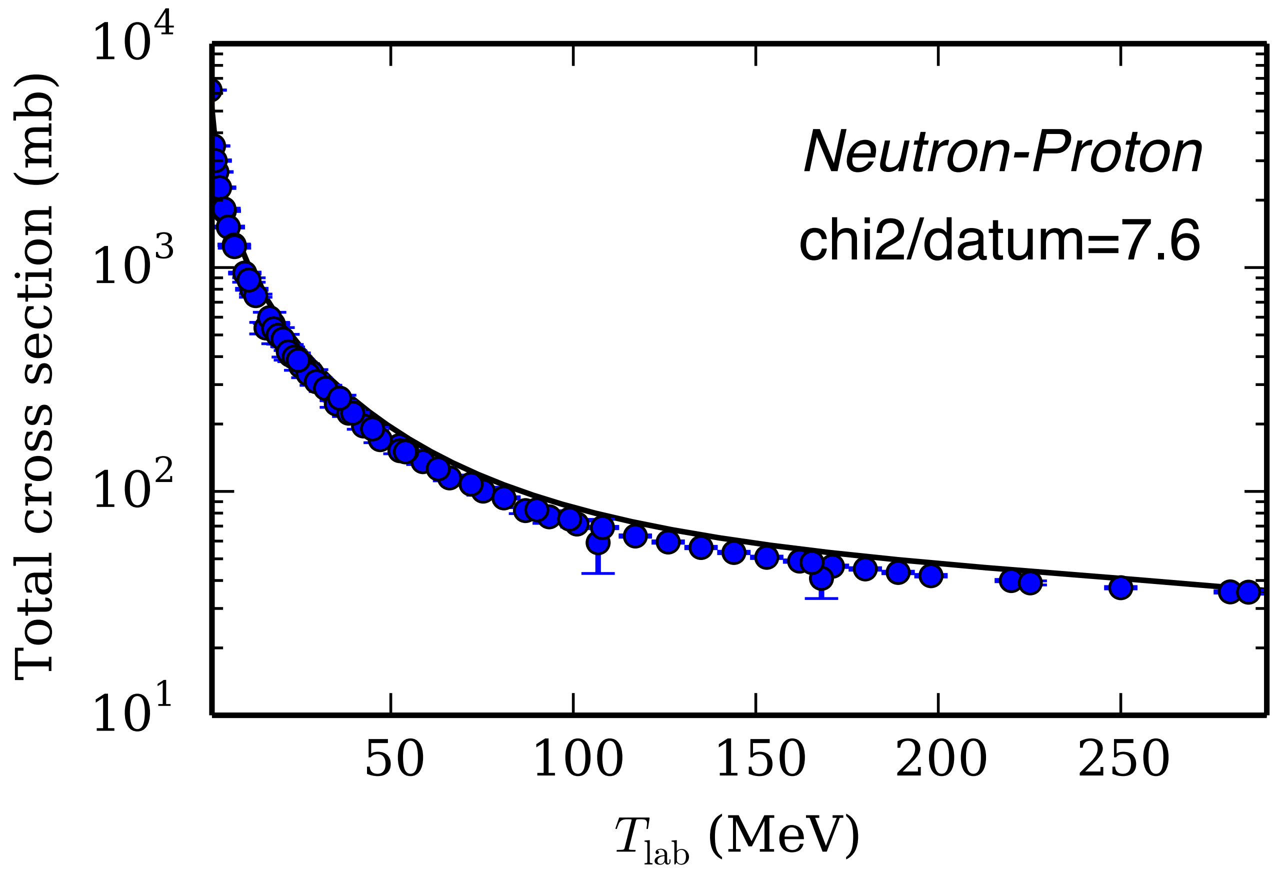

Nucleon-nucleon cross sections

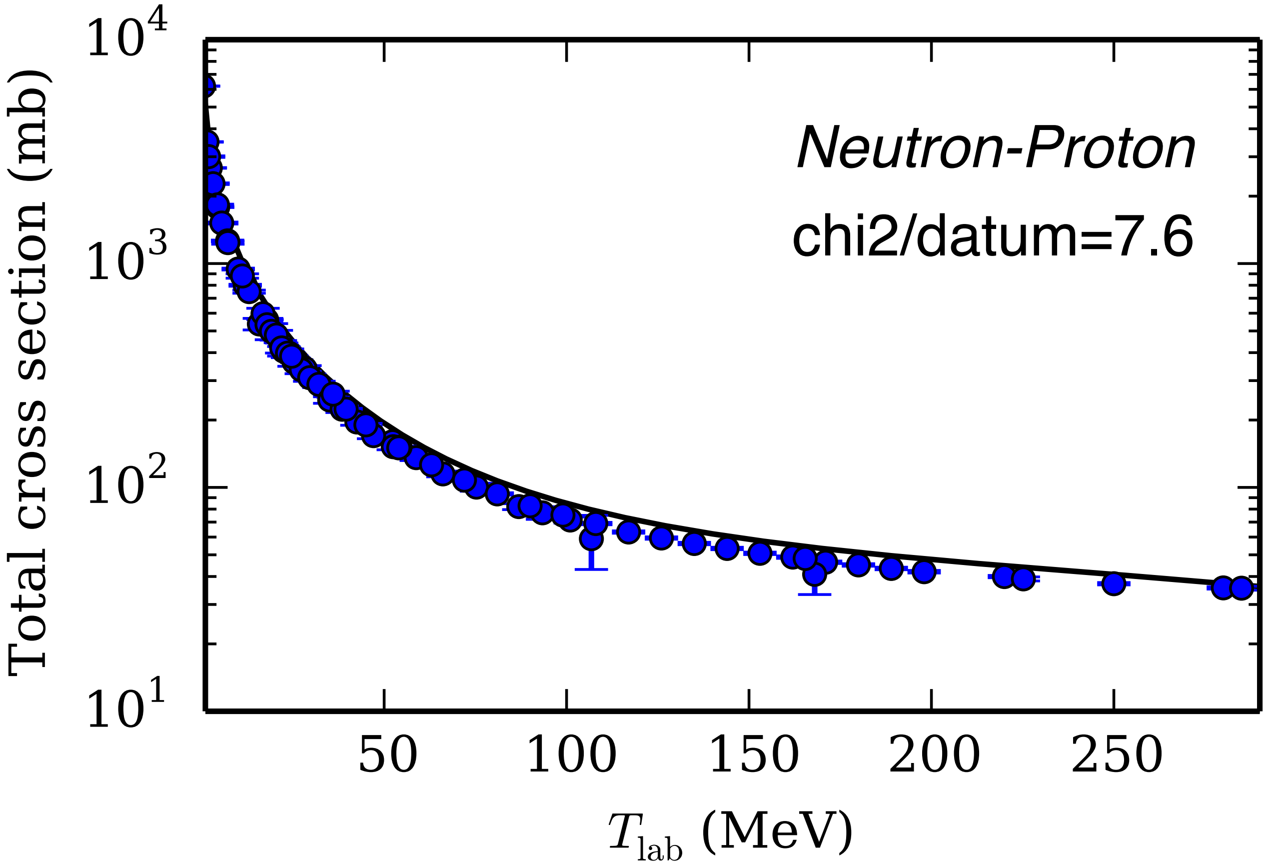

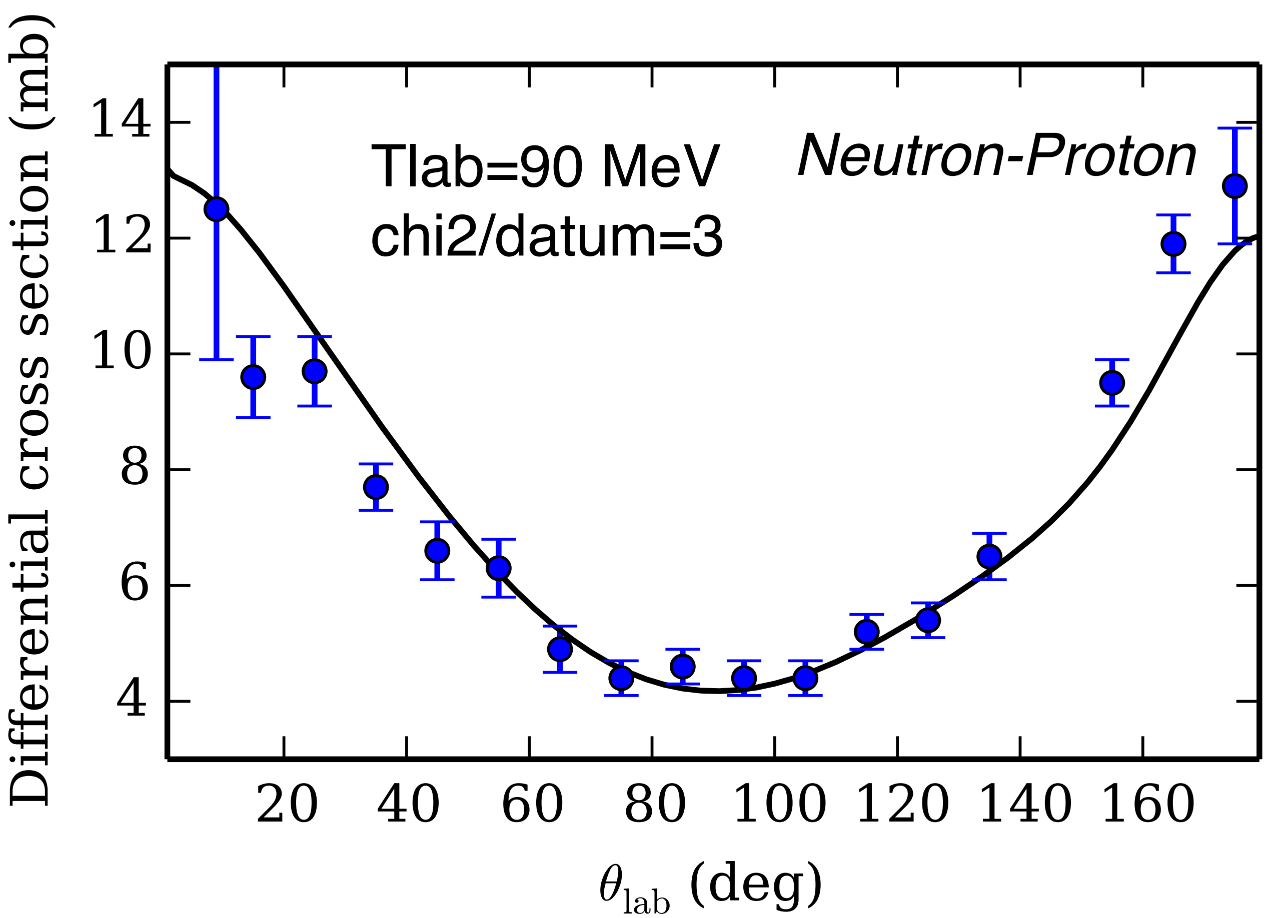

Nucleon-nucleon cross sections

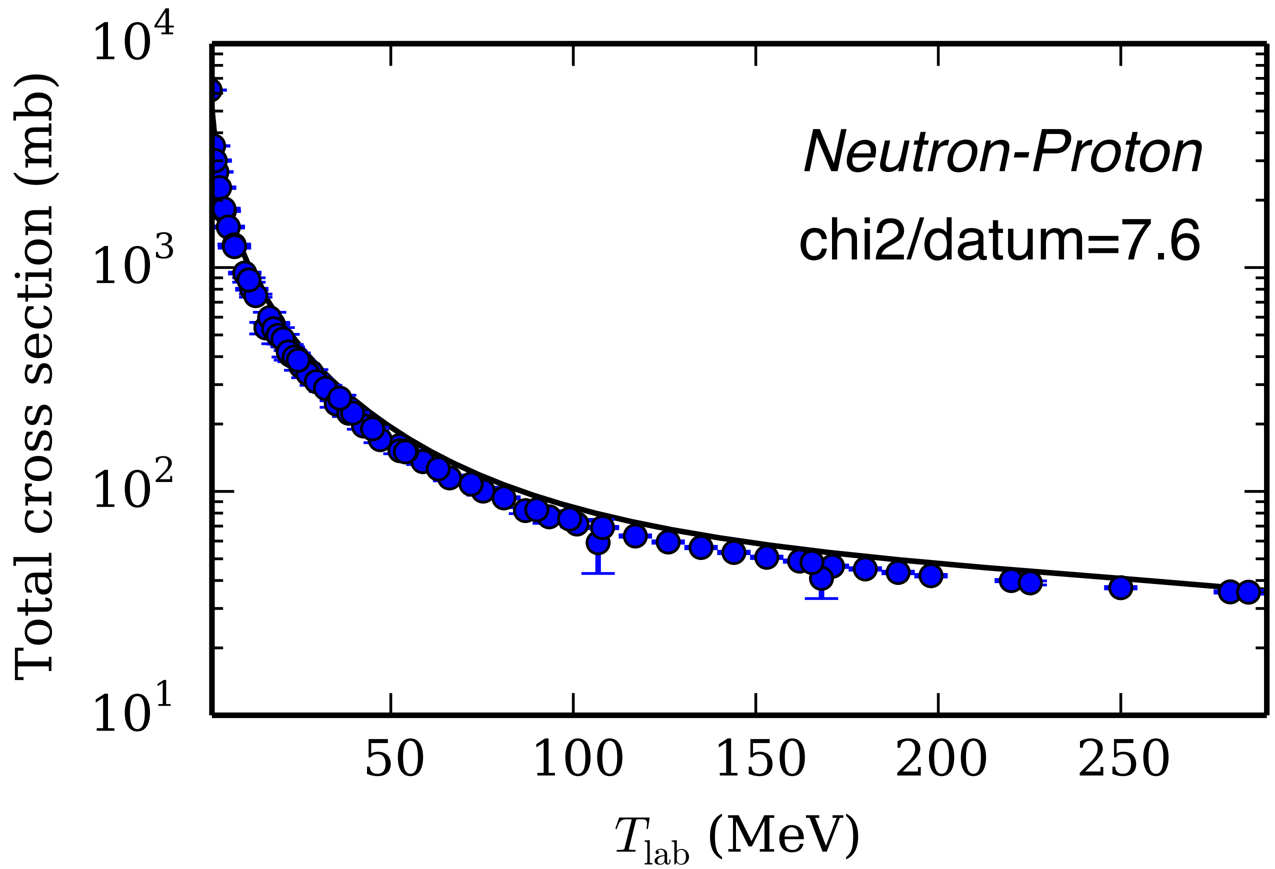

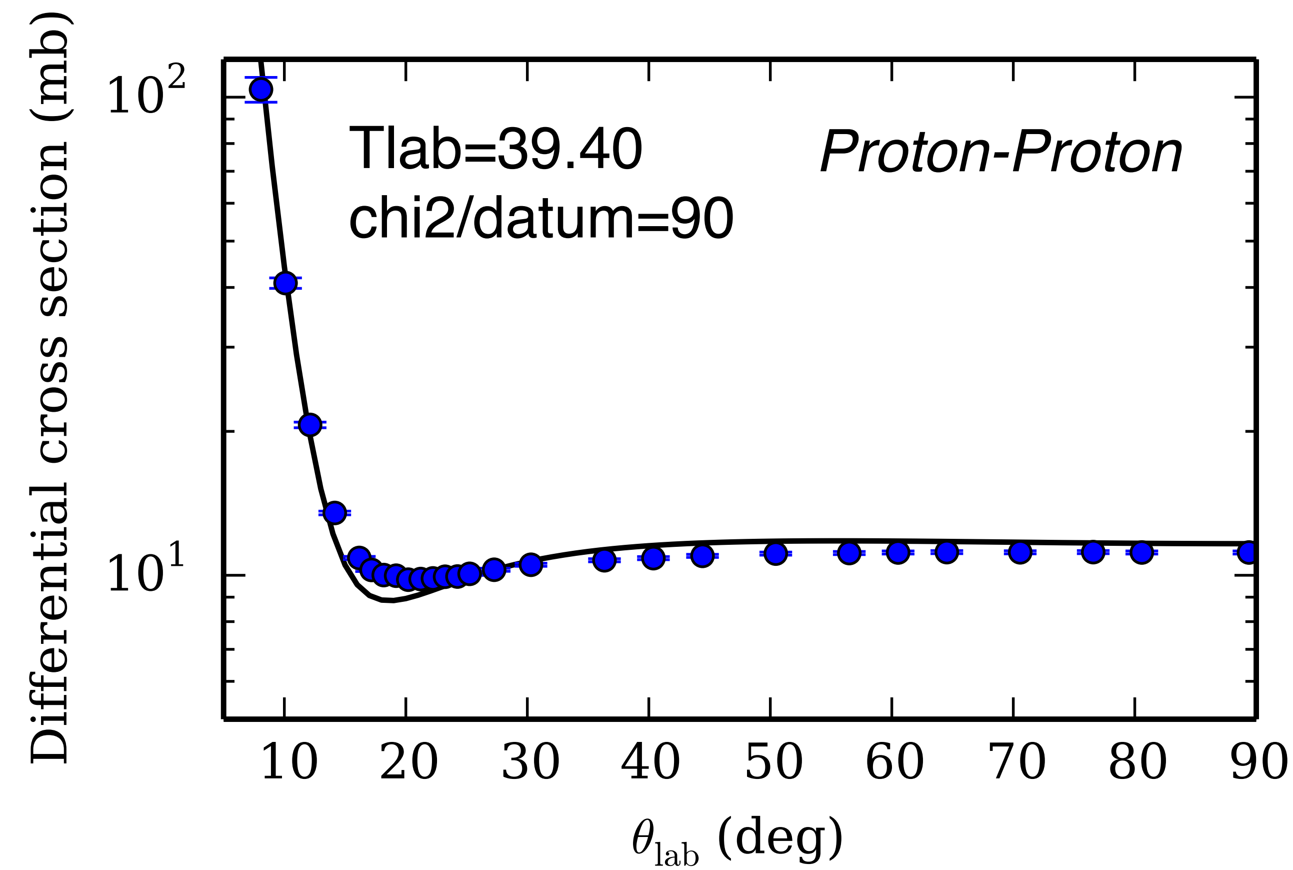

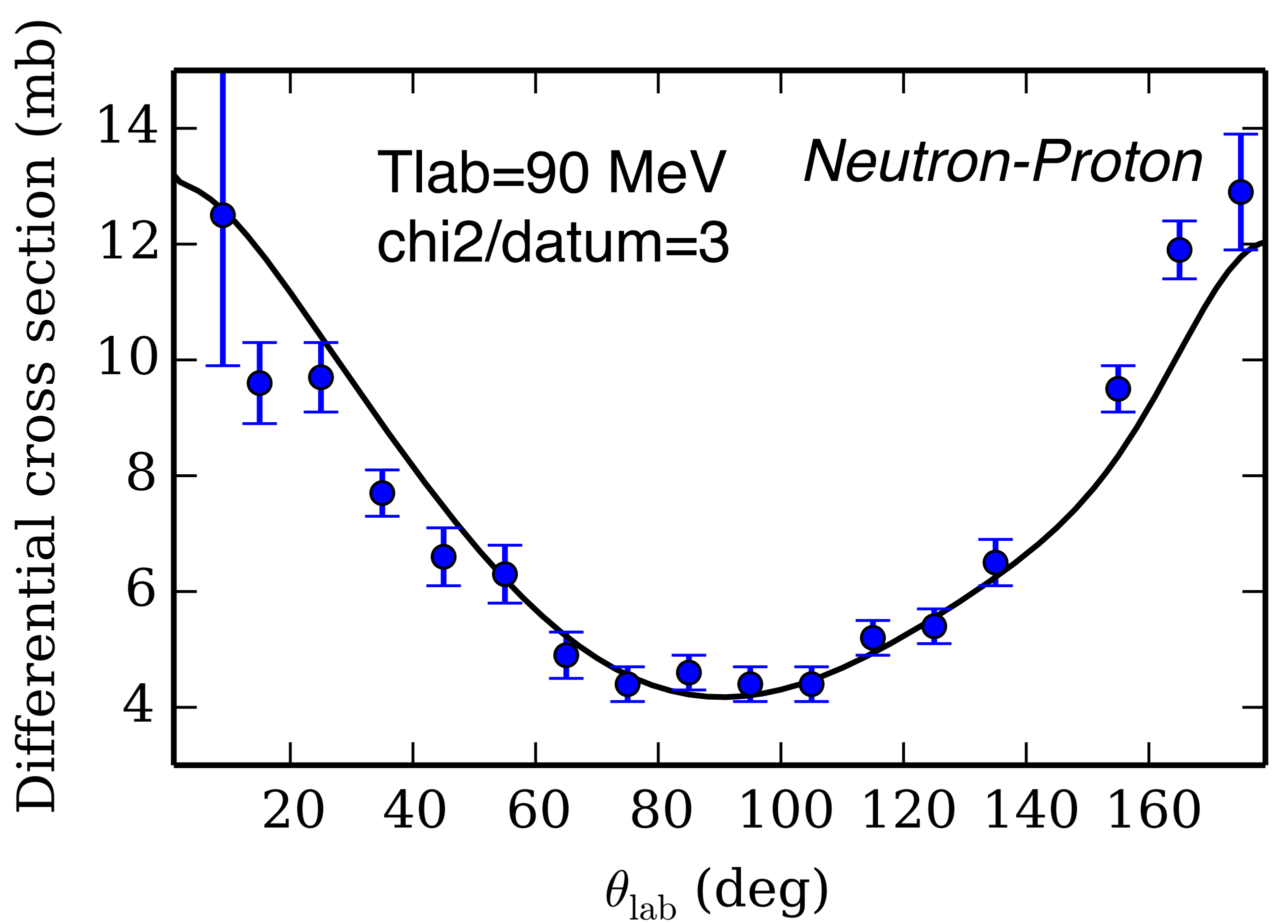

Nucleon-nucleon cross sections

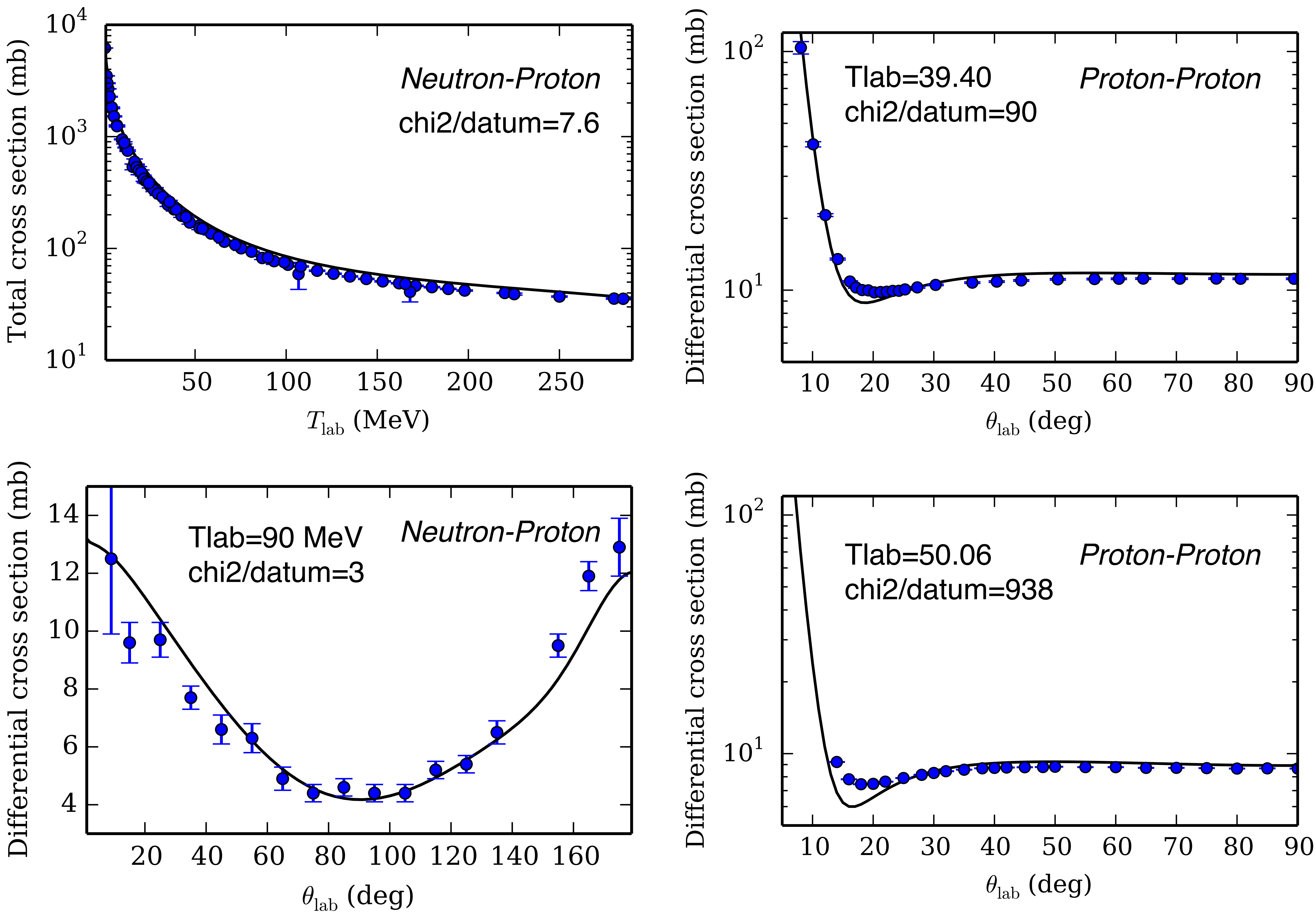

Low Energy Coupling constants

Parameter	$NNLO_{opt}$	$NNLO_{sat}$
c1	-0.92	-1.12
c3	-3.89	-3.93
c4	4.31	3.77
cD	—	0.82
cE	—	-0.04

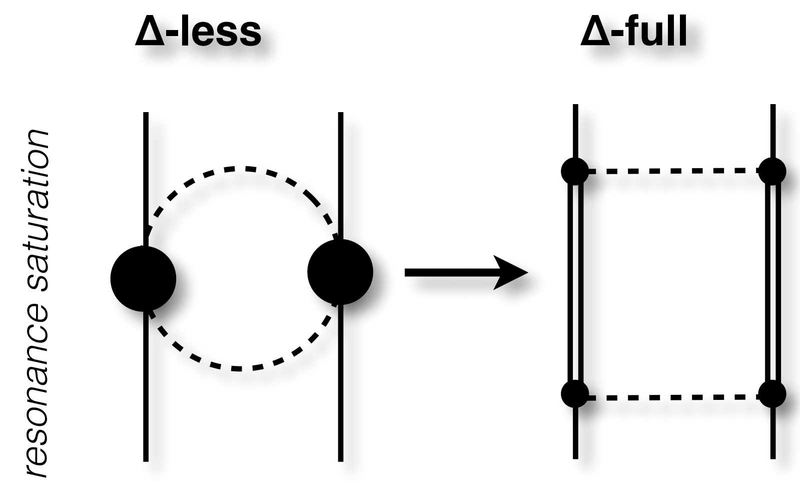

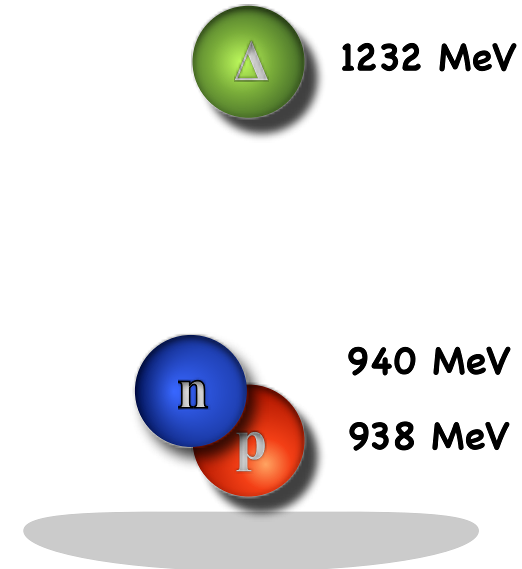

Low Energy Coupling constants

Parameter	$NNLO_{opt}$	$NNLO_{sat}$
c1	-0.92	-1.12
c3	-3.89	-3.93
c4	4.31	3.77
cD	—	0.82
cE	—	-0.04

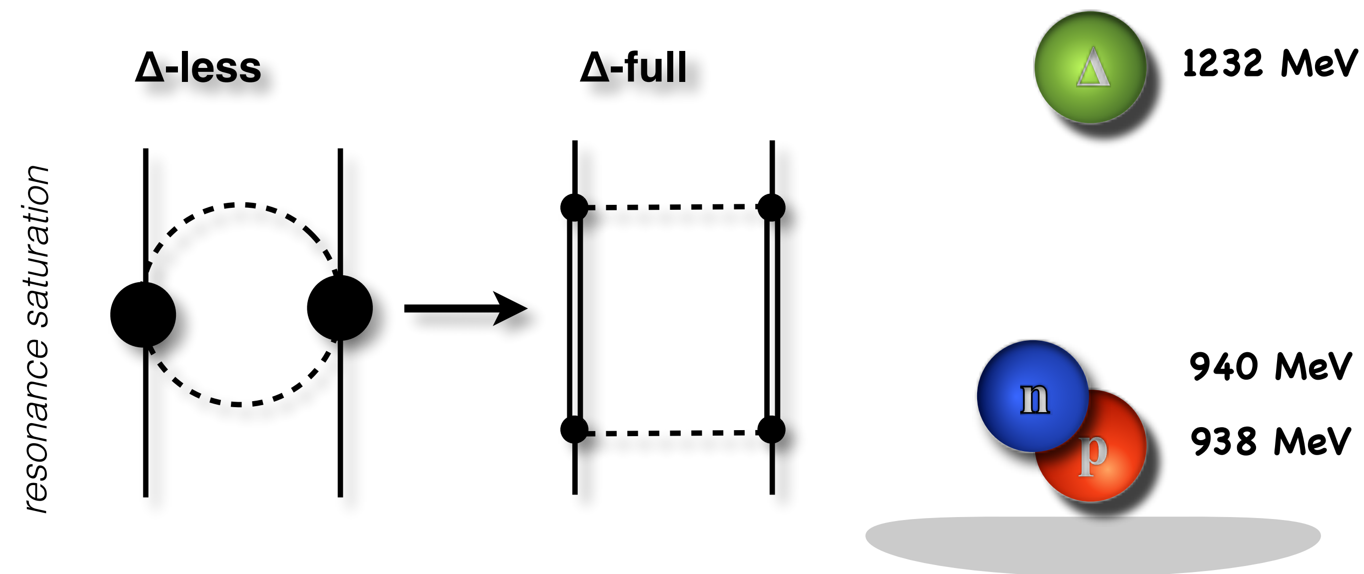

piN-Krebs: fourth order, pLab=150 MeV [GW06,KH86]
piN-BM: third order, pLab=40-97 MeV [KA84]
NN-PWA: Nijmegen PWA, 0-350 MeV
NNLO: piN-BM, but c3 chosen on the larger side
N3LO(Idaho): piN-BM, but c3, and c4 chosen on the larger side
NNLOopt: Guided by fit to NN data
Wendt: optimized, fourth order, pLab=150 MeV [GW06].

	piN-Krebs	piN-BM	NN-PWA	NNLO (Juelich)	N3LO (Idaho)	NNLOopt	Wendt
c1	[-1.13,-0.75]	-0.81±0.12	-0.76±0.07	-0.81	-0.81	-0.92	-1.40±0.12
c3	[-5.51,-4.77]	-4.70±1.16	-4.78±0.10	-3.4	-3.2	-3.89	-4.56±0.11
c4	[3.34,3.71]	3.40±0.04	+3.96±0.22	+3.40	+5.40	+4.31	3.72±0.27

^{16}O charge density and negative parity states

Charge density

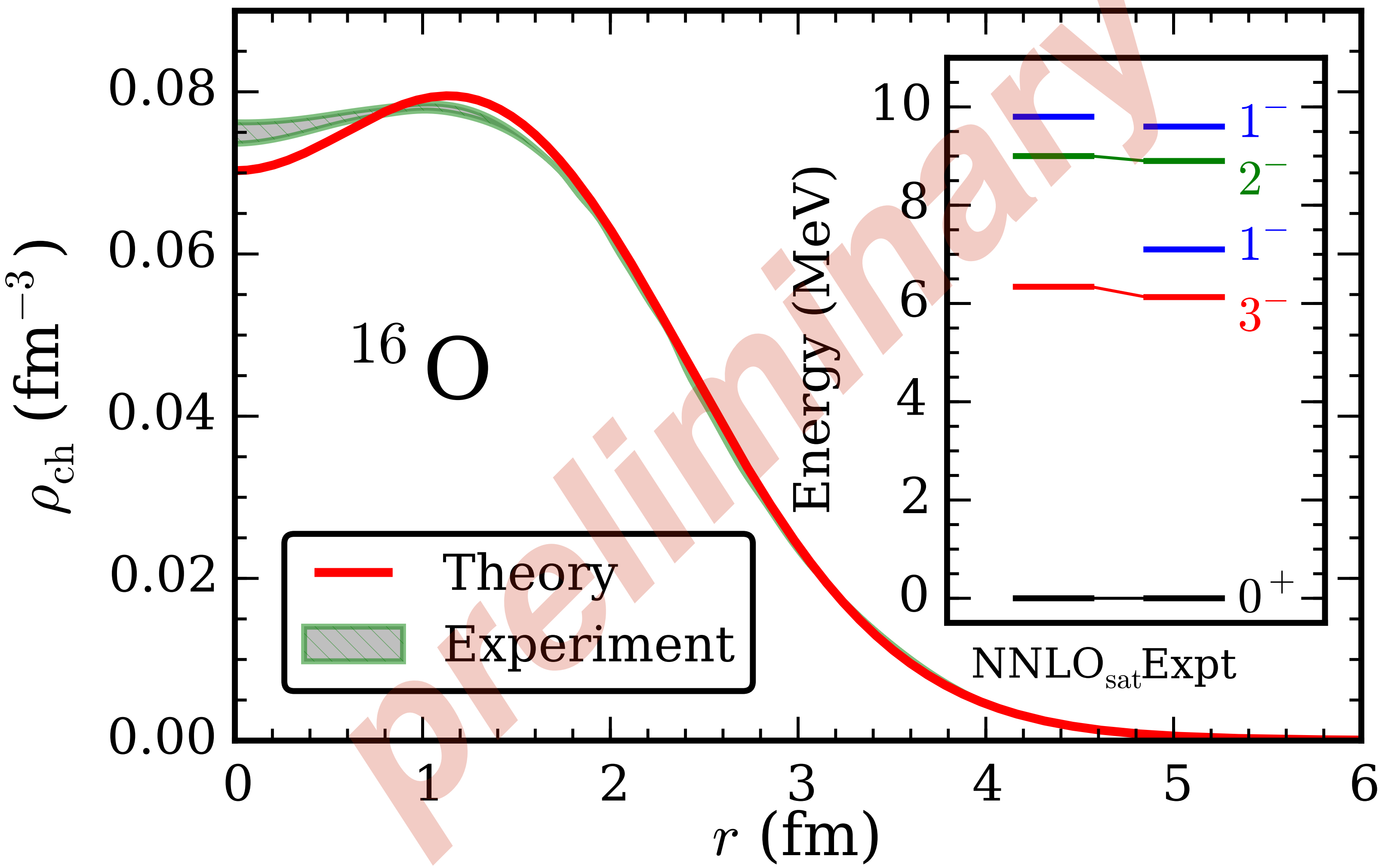

One-nucleon separation energies

	NNLOsat	Experiment
$S_n(^{17}O)$	4.0 MeV	4.14 MeV
$S_n(^{16}O)$	14.0 MeV	15.67 MeV
$S_p(^{17}F)$	0.5 MeV	0.60 MeV
$S_p(^{16}O)$	10.7 MeV	12.12 MeV

Λ-CCSD(T)
hw=22 MeV, Nmax=14
E3max=16
NO2B HF basis
+leading order
NNN contribution
to the total energy

ab initio challenge:
E(3^-)=6.34 MeV

NNLOsat
E(3^-)=6.13 MeV, 90%
1p-1h excitation ($p_{1/2}$-$d_{5/2}$)

Suggesting that the 1^-_2 and 2^-_1 states also are of 1p-1h character

1p-1h states sensitive to the particle-hole gap (A=16/17 separation energies)

Experimental charge distribution data: H. DeVries, et al At. Data Nucl. Data Tables 36, 494 (1987)

Spectra, binding energies and radii

preliminary

Λ-CCSD(T)
hw=22 MeV, Nmax=14
E3max=16
NO2B HF basis
+leading order
NNN contribution
to the total energy

Ground state energies in MeV:

		$NNLO_{sat}$	Exp.
NCSM	^{6}Li	32.4	32.0
	^{8}He	30.9	31.5
	^{9}Li	43.9	45.3
	^{14}N	103.7	104.7
	^{22}F	163.0	167.7
	^{24}F	175.1	179.1

Radii in fm:

	charge	matter	Exp.
^{8}He	1.91	—	1.959(16)
^{9}Li	2.22	—	2.217(35)
^{22}O	(2.72)	2.80	2.75(15)
^{24}O	(2.76)	2.95	—

^{18}O spectra compressed
$E(2^{+})$=0.7 MeV (exp. 1.9 MeV)

Spectra, binding energies and radii

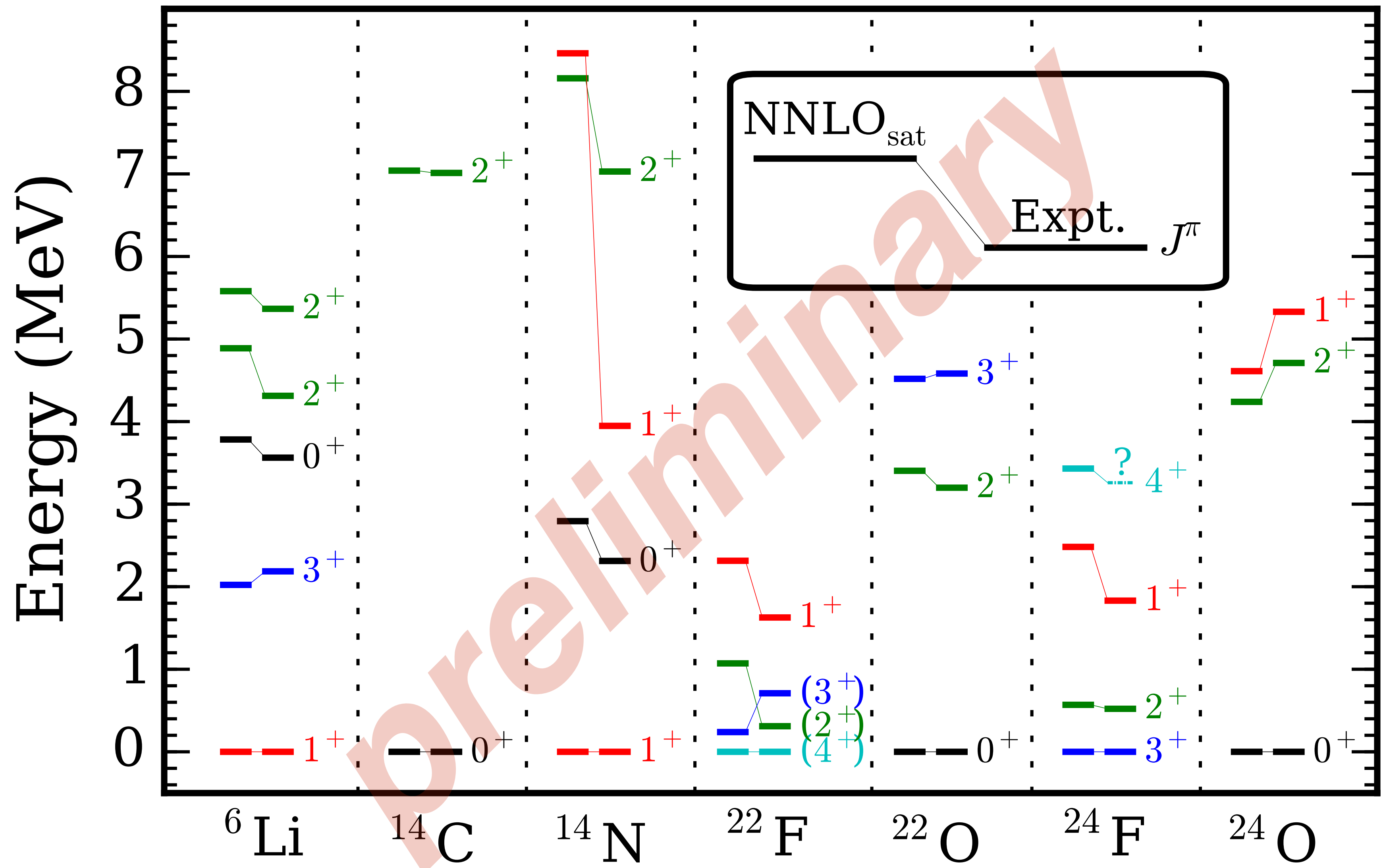

Λ-CCSD(T)
hw=22 MeV, Nmax=14
E3max=16
NO2B HF basis
+leading order
NNN contribution
to the total energy

Ground state energies in MeV:

		$NNLO_{sat}$	Exp.
NCSM	^{6}Li	32.4	32.0
	^{8}He	30.9	31.5
	^{9}Li	43.9	45.3
	^{14}N	103.7	104.7
	^{22}F	163.0	167.7
	^{24}F	175.1	179.1

Radii in fm:

	charge	matter	Exp.
^{8}He	1.91	—	1.959(16)
^{9}Li	2.22	—	2.217(35)
^{22}O	(2.72)	2.80	2.75(15)
^{24}O	(2.76)	2.95	—

^{18}O spectra compressed
$E(2^{+})$=0.7 MeV (exp. 1.9 MeV)

Spectra, binding energies and radii

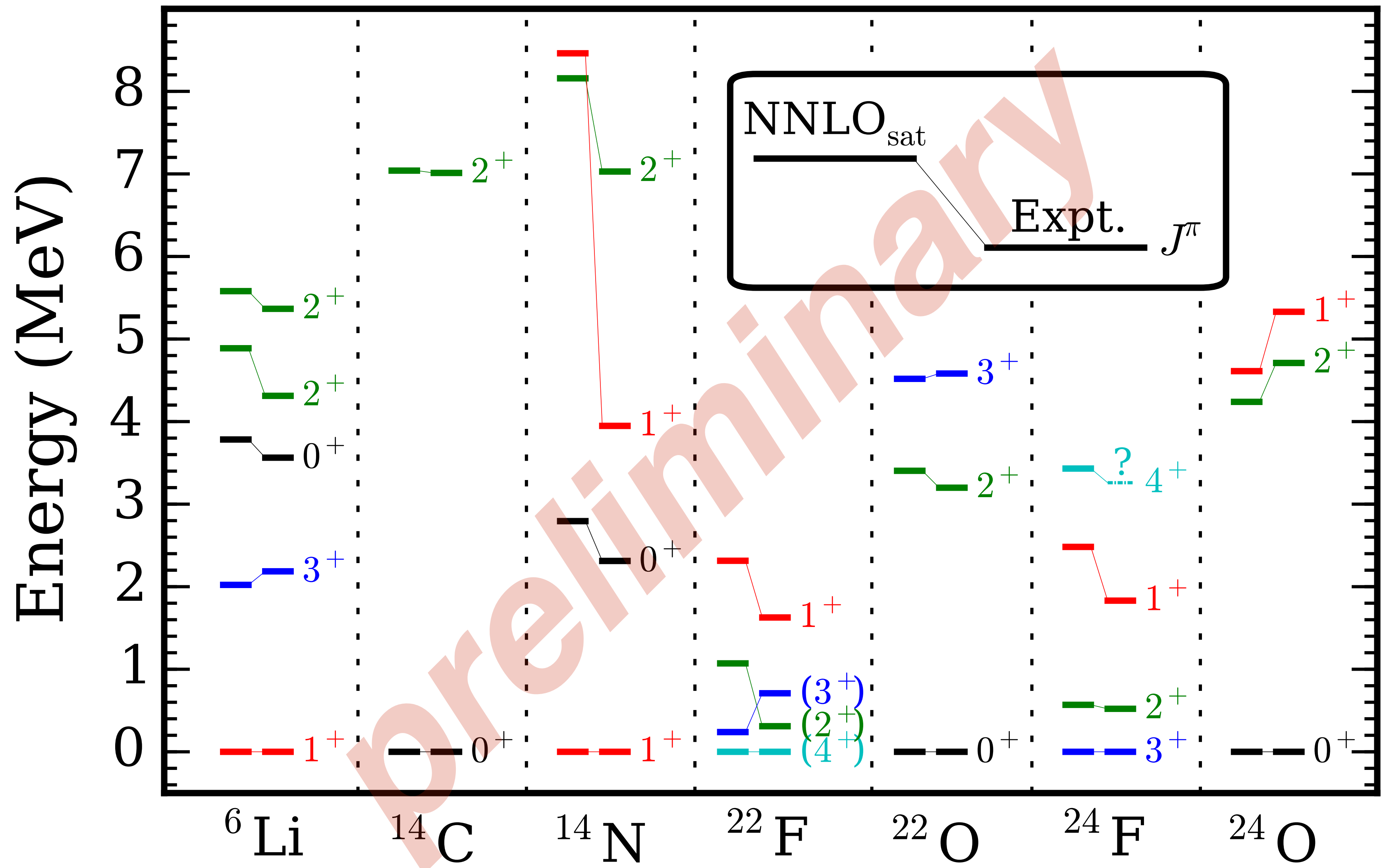

Calcium-40

	E_{gs} (MeV)	r_{ch} (fm)	E(3^-) (MeV)
NNLOsat	326	3.48	3.81
Experiment	342	3. 48	3.74

Λ-CCSD(T)
hw=22 MeV, Nmax=14
E3max=16
NO2B HF basis
+leading order
NNN contribution
to the total energy

Ground state energies in MeV:

		NNLO$_{sat}$	Exp.
NCSM	^{6}Li	32.4	32.0
	^{8}He	30.9	31.5
	^{9}Li	43.9	45.3
	^{14}N	103.7	104.7
	^{22}F	163.0	167.7
	^{24}F	175.1	179.1

Radii in fm:

	charge	matter	Exp.
^{8}He	1.91	—	1.959(16)
^{9}Li	2.22	—	2.217(35)
^{22}O	(2.72)	2.80	2.75(15)
^{24}O	(2.76)	2.95	—

^{18}O spectra compressed
E(2^+)=0.7 MeV (exp. 1.9 MeV)

NNLO$_{sat}$ and symmetric nuclear matter

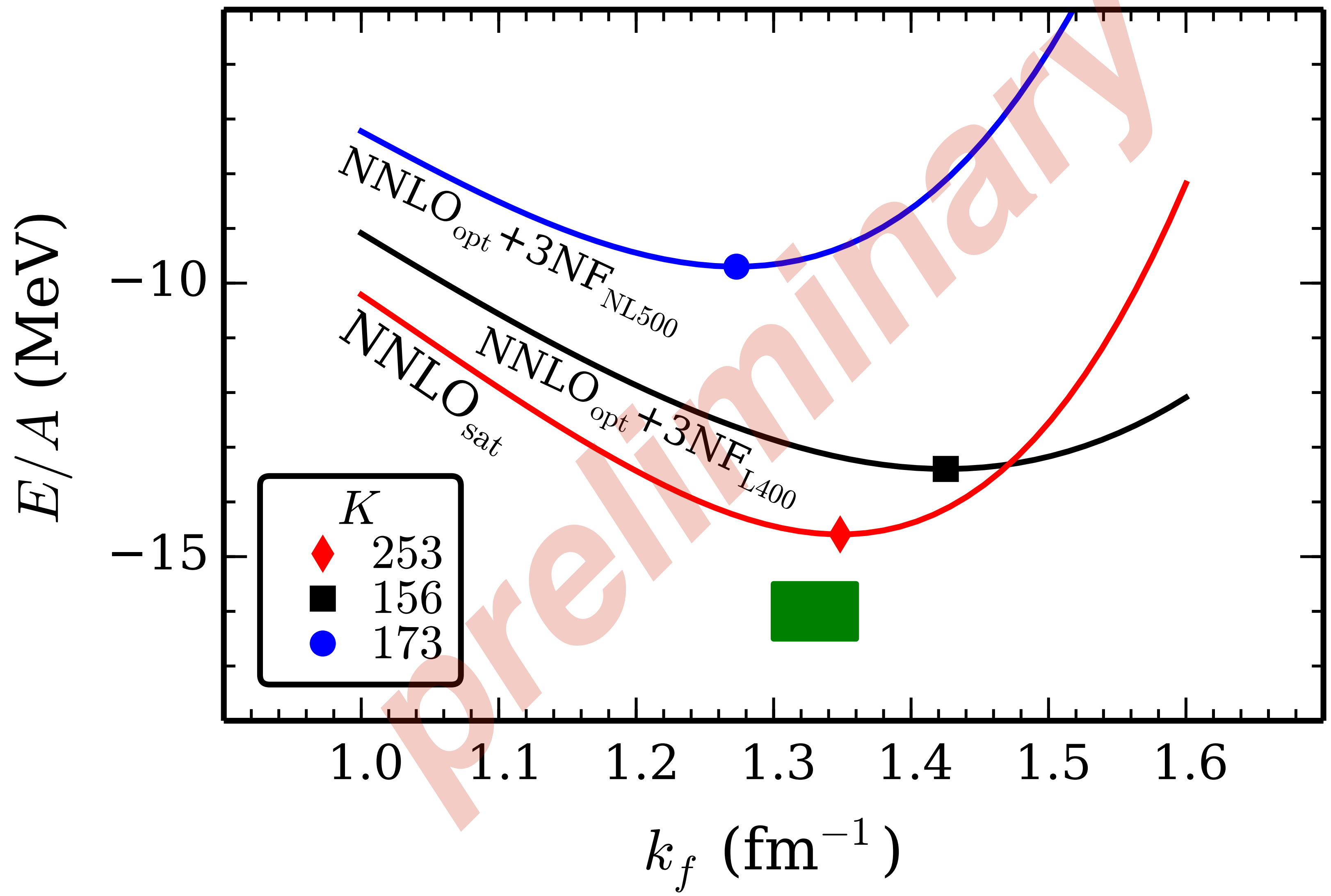

Coupled-cluster calculations of nucleonic matter

G. Hagen et al.

PHYSICAL REVIEW C 89, 014319 (2014)

NNLO$_{sat}$ saturation properties

E/A = -14.59 MeV
k_f = 1.35 fm-1
ρ_0 = 0.17 fm-3

incompressibility

$$K = 9\rho_0^2 \frac{d^2(E/A)}{d\rho^2}\bigg|_{\rho=\rho_0}$$

inversely proportional to the compressibility.

cannot be measured directly, but related to e.g. the giant monopole resonance ('breathing mode') in finite nuclei.

J. P. Blaizot Phys. Rep. 64, 171 (1980)

NNLO_{sat} and symmetric nuclear matter

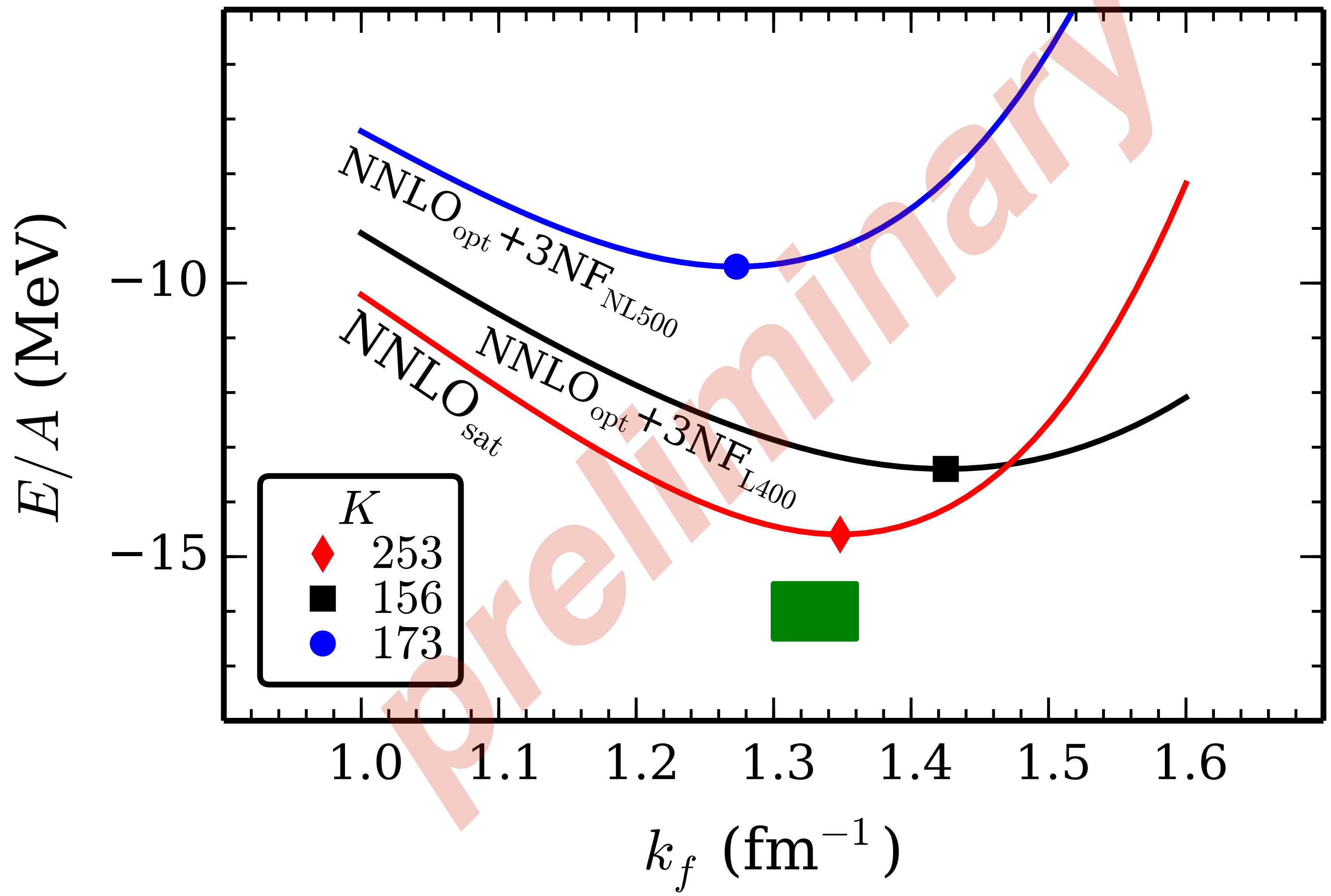

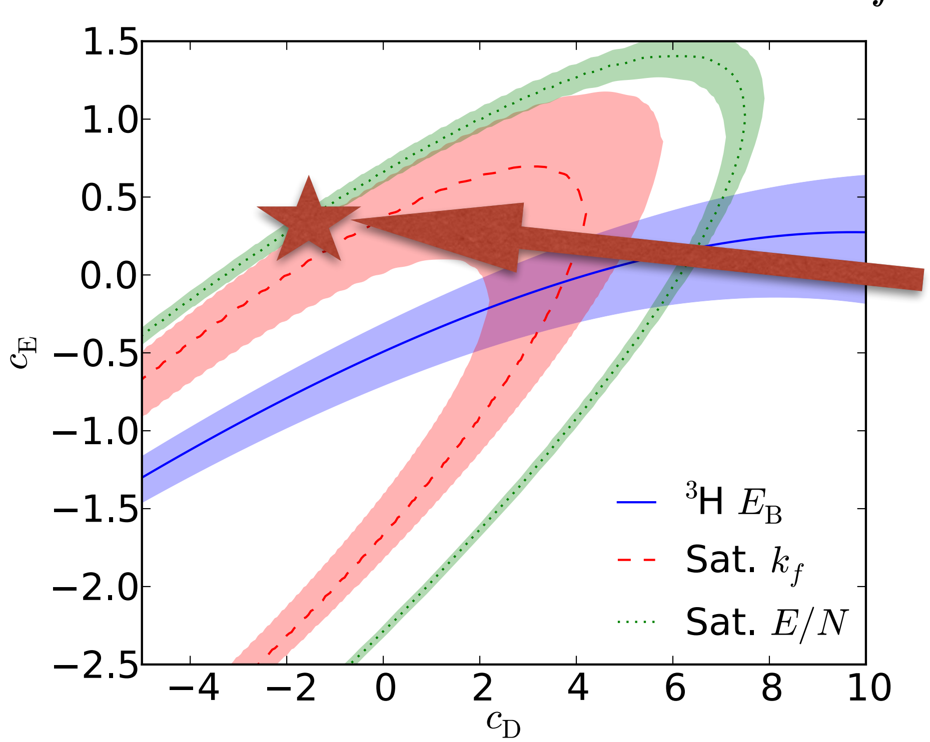

NNLO_{opt} + $3\text{NF}_{\text{NL500}}$:

E/A=-15.5 MeV & k_f=1.4 fm^{-1}
^{3}H =-13.5 MeV (!)

Simultaneous optimization is key!

Coupled-cluster calculations of nucleonic matter

G. Hagen et al.

PHYSICAL REVIEW C 89, 014319 (2014)

NNLO_{sat} saturation properties

E/A = -14.59 MeV
k_f = 1.35 fm-1
ρ_0 = 0.17 fm-3

incompressibility

$$K = 9\rho_0^2 \frac{d^2(E/A)}{d\rho^2}\bigg|_{\rho=\rho_0}$$

inversely proportional to the compressibility.

cannot be measured directly, but related to e.g. the giant monopole resonance ('breathing mode') in finite nuclei.

J. P. Blaizot Phys. Rep. 64, 171 (1980)

Summary and conclusions

- *$NNLO_{sat}$ Accurately reproduces the binding energies and charge radii for many light- and medium-mass nuclei, most importantly $^{40,48}Ca$.*
- *$NNLO_{sat}$ almost reproduces the empirical saturation of symmetric nuclear matter.*
- *Spectra of most isotopes are very reasonable, and certainly not worse than with other state-of-the-art chiral potentials.*
- *During development, Λ=475, 500 MeV were also employed. This led to similar results.*
- *The next step is the optimization of N3LO NN+3NF.*
- *Finally, much effort is going into estimating the uncertainty budget of chiral interactions and many-body calculations.*